

## CHAPTER VI

### STUDIES ON BINARY MIXTURES WHICH EXHIBIT A MAXIMUM AS WELL AS A MINIMUM IN THE A-N TRANSITION BOUNDARY

#### 6.1 Introduction

Studies on binary mixtures of mesomorphic compounds have been of considerable interest, For example, in the identification of mesophase types. When two nematogens are mixed together, usually the mixtures exhibit only the nematic phase.  $T_{NI}$ , the nematic-isotropic transition temperature of such mixtures varies linearly with composition to a good approximation.<sup>1-8</sup> In such systems, the dependence of the melting point of the solid on the composition can be described by the Schröder-Van Laar equation.<sup>9</sup>

However, in the recent past, new types of phase diagrams have been found in binary mixtures of some nematogens.<sup>10-20</sup> These mixtures show the smectic A phase (and sometimes other smectics) in some range of compositions (medium concentrations) even when neither component in the pure state exhibits the smectic A phase. Confining our attention to such an 'induced smectic A'

phase (or induced A phase), the A-N transition boundary characteristically exhibits a maximum for a certain composition which is usually 50 mole% of the components (fig. 1a,b).<sup>6</sup> It is now known that the induced A phase is observed in some composition range of the mixtures when one of the components has the strongly polar cyano or nitro end group while the other component has no such group. Thus interactions between permanent dipole moment of the strongly polar molecule and the induced dipole moment of the weakly polar molecule appear to be important for the occurrence of the induced A phase. We must, however, mention that Demon and Billard<sup>21</sup> and Suresh<sup>22</sup> have found the induced A phase in some systems even when neither component has the cyano or nitro end group.

Park et al<sup>13</sup> suggested that induced A phase is formed by virtue of a charge transfer interaction of the components of a binary mixture containing strongly polar and weakly polar molecules. In such mixtures, charge transfer complex formation takes place between the molecules of the two kinds, the highly polar component acting as the acceptor while the other component acts like a donor. Evidence for such an interaction has been found by Sharma et al<sup>23</sup> who detected an additional absorption band with negative dichroism in the visible/UV

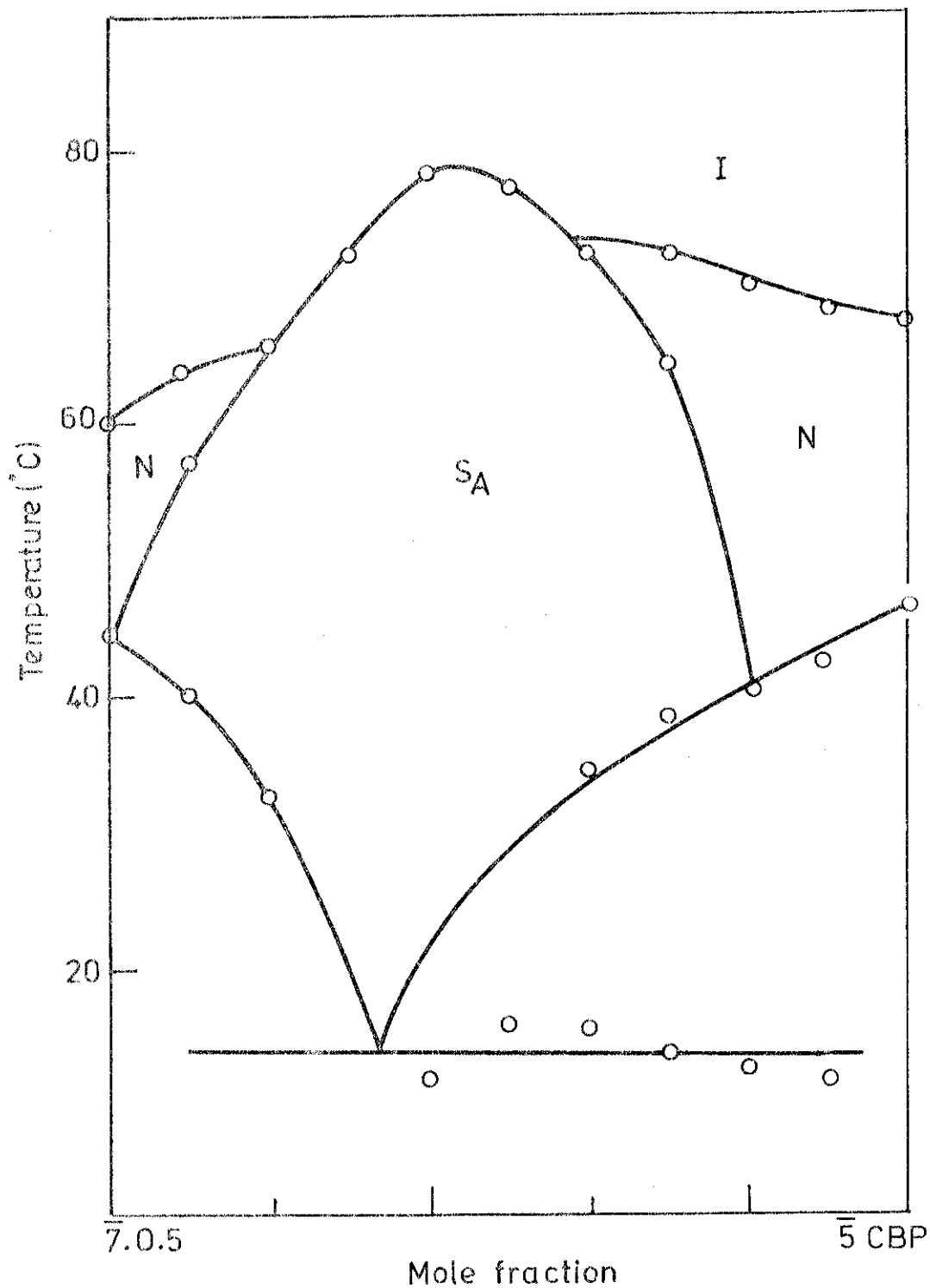


**FIG.6.1a:** Phase diagram of the binary system: 4-n-pentyl-phenyl-4'-n-heptyloxybenzoate (7.0.5) and 4-n-pentyloxy-4'-ayenobiphenyl (5 CBP). (Reproduced from ref.16)

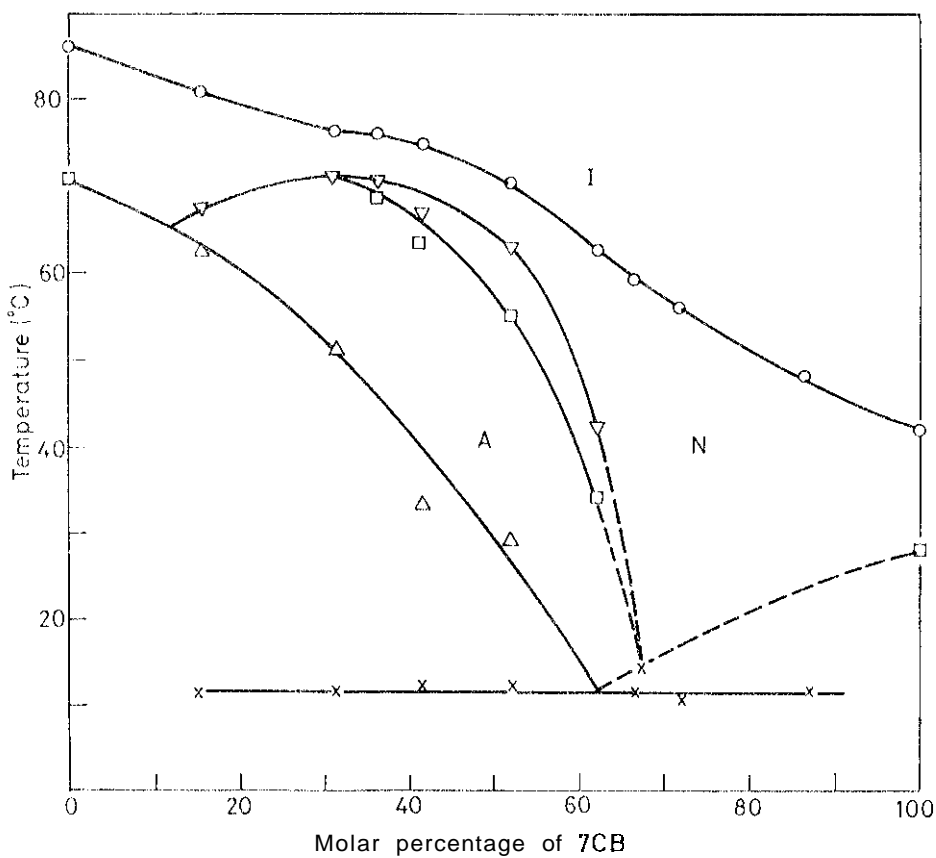


**FIG. 6. 1b:** Phase diagram of mixtures of (2-hydroxy)p-ethoxybenzylidene-p'-butylaniline (OH-EBBA) with 4'-n-heptyl-4-cyanobiphenyl (7CB). (Reproduced from ref. 17).

spectrum of some mixtures exhibiting the induced A phase. This interaction results in a strong lateral attraction between the two types of molecules and in turn can lead to the formation of a layered arrangement characteristic of smectic phases.

As discussed in the earlier chapters (I, III and IV), the A phase exhibited by highly polar compounds will be of a bilayer variety, the layer spacing being considerably greater than the molecular length.<sup>24</sup> This structure arises due to the strong antiparallel correlations between the neighbouring molecules of terminal polar compounds.<sup>25</sup> In binary mixtures of such compounds with weakly polar compounds, it is found in some cases that the bilayer smectic is immiscible with the induced A phase<sup>26</sup> (fig.6.2). If the bilayer corresponds to nearly two molecular lengths (i.e., A<sub>2</sub> phase), one gets a phase transition from a bilayer A phase to a monolayer A phase (A<sub>1</sub> phase) (as discussed in chapter I ).<sup>27</sup>

The antiparallel correlations between the molecules of the polar component on one hand, and the charge transfer complex formation between the two types of molecules on the other lead to significant influences on the physical properties of the mixtures. For example, Park et al<sup>13</sup> have observed strong positive deviations in



the value of dielectric anisotropy ( $\Delta\epsilon$ ). A 50-50 mole per cent of N-(p-methoxybenzylidene)-p-n-butylaniline (MBBA) and 4-cyano-4'-pentylbiphenyl (CPB) has a  $\Delta\epsilon$  of 7.7 whereas a simple additive law implies a value of 5.8. The interactions also cause changes in viscosities and elastic constants of the mixtures.<sup>28</sup>

As we saw in the previous chapter, smectic-like short range order in the medium influences conductivity anisotropy to a considerable extent. Bock et al<sup>29</sup> have measured the electrical conductivity of two liquid crystal mixtures exhibiting induced A phases. Their results show that conductivity anisotropy of the mixtures, which is negative at lower concentrations of the polar component, increases and becomes positive with increasing concentration of the polar component. They have attributed this to the growing bilayer structure of the polar component.

From the above discussion it is clear that specific molecular interactions influence the physical properties of the mixtures considerably. We have studied several binary mixtures which exhibit the induced A phase or a nematic gap between  $A_g$  and induced phases.

### Examples for systems exhibiting induced A phase

- 1 4-cyanophenyl-3'-methyl-4'-(4"-n-dodecylbenzoyloxy) benzoate (12 CPMBB) and 4-biphenyl-4"-n-undecyloxy benzoate (BO11).
- 2 (2-hydroxy)-p-ethoxybenzylidene-p'-butylaniline (OH-EBBA) and p'-n-octyloxy-p-cyanobiphenyl (8 OCB).
- 3 BO11 and p'-nitrophenyl-p-n-octyloxybenzoate (NFOOB).
- 4 BO11 and N-(p-cyanobenzylidene)-p'-octyloxyaniline (CBOOA).

### Examples for systems exhibiting a nematic gap

- 1 CBOOA and OH-EBBA
- 2 trans-4-propylcyclohexyl-4-(trans-4-pentylcyclohexyl) benzoate and CBOOA.
- 3 8 OCB and trans-4-propylcyclohexyl-4-(trans-4-pentyl cyclohexyl)benzoate.

Of these, we have undertaken a systematic study of phase diagrams, temperature variations of layer spacings, static dielectric constants, dielectric relaxation and conductivities of several mixtures of two binary systems. These mixtures exhibit a well defined minimum as well as a maximum (indicative of induced A phase) in the smectic A - nematic (A-N) transition boundary. The results are discussed in this chapter.



## **6.2 Experimental**

The two components of the mixture were weighed accurately (using an autobalance Perkin Elmer Model AD-2) into a glass cup provided with a ground glass stopper. The mixture was heated to the isotropic phase and mixed thoroughly by mechanical stirring. Then it was kept in the isotropic phase for a few hours. The sample was then transferred on to a slide while it was in the isotropic phase. The transition temperatures were determined by using a Mettler hot-stage (FP-52) in conjunction with a polarizing microscope. The rates of heating and cooling used for this purpose were  $0.2^{\circ}/\text{minute}$ . These transitions were also confirmed using a differential scanning calorimeter (Perkin-Elmer DSC-2). Heats of transitions of various mixtures were also determined from the DSC studies.

The experimental techniques for the measurement of layer spacings, static dielectric constants, dielectric dispersion and conductivities have already been described in the previous chapters.

## **6.3 Results and discussion**

### **(a) Phase diagram studies**

The two binary systems investigated are:

(5) p'-nitrophenyl-p-n-octyloxybenzoate (NPOOB) with (2-hydroxy)-p-ethoxybenzylidene-p'-butylaniline (OH-EBBA) and (ii) p'-n-octyloxy-p-cyanobiphenyl (S OCB) with p-butoxyphenyl-(p'-pentyloxy)benzoate (40.05). S OCB was bought from Hoffmann-La Roche and used without further purification. 40.05 and OH-EBBA were synthesized in our chemistry laboratory and the NPOOB sample was kindly sent to us by Prof. A.C.Griffin.

The structural formulae of all the compounds are shown in fig.6.3.

1) Mixtures of NPOOB and OH-EBBA (System I): The phase diagram of the mixtures is shown in fig. 6.4. NPOOB has the strongly polar nitro end group and exhibits a partially bilayer A phase ( $A_d$ ) with layer spacing  $\approx 1.2l$ , where  $l$  is the molecular length. OH-EBBA shows only a nematic phase. The system exhibits a pronounced maximum in the A-N boundary, indicative of an induced A phase. The peak in the A-N boundary is observed for medium concentrations ( $\sim 50\%$  of the polar component). This agrees with several earlier observations<sup>10-20</sup> (see fig.6.1a,b). The N-I transition curve is also influenced by the A-N boundary as can be seen from the diagram. More interestingly, the A-N boundary exhibits a well

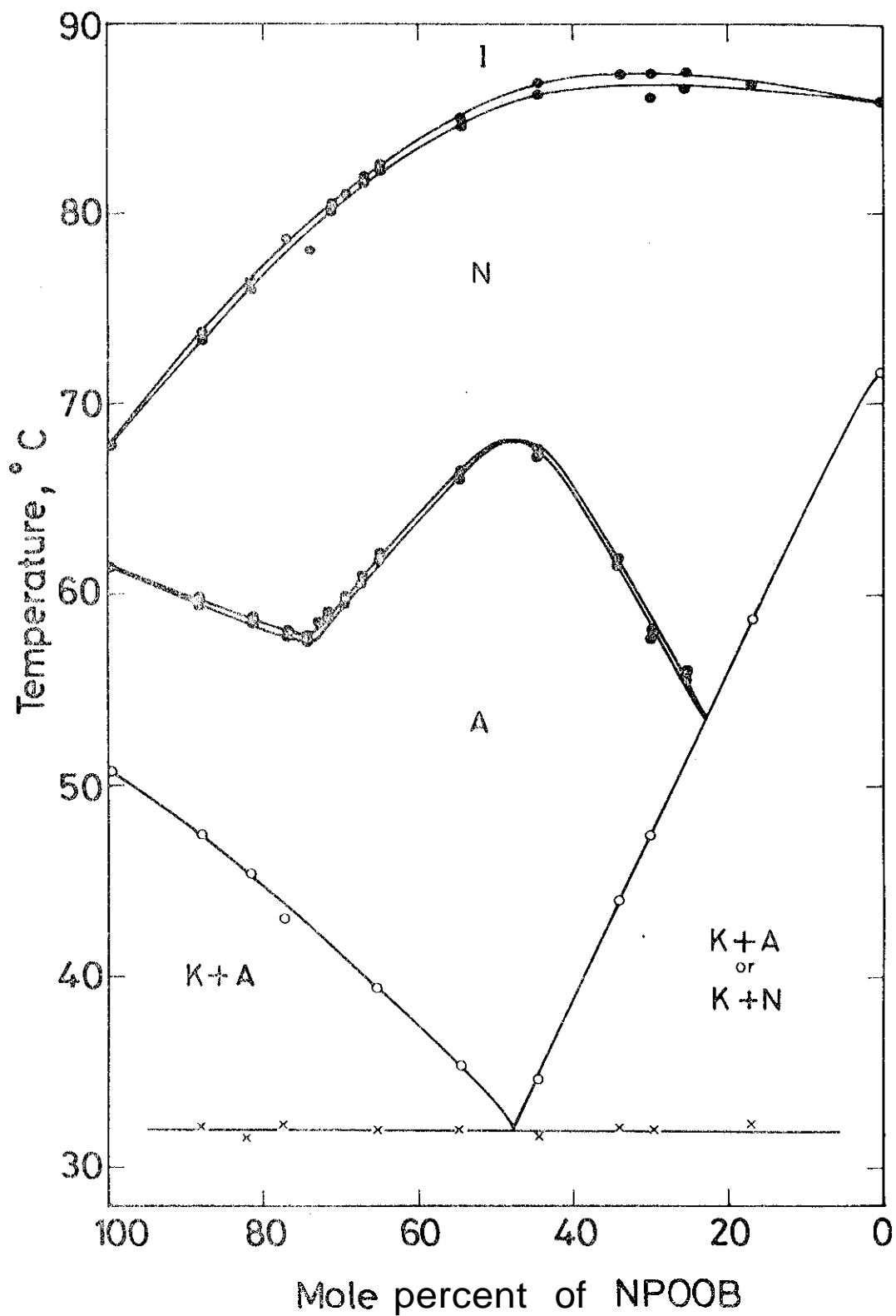
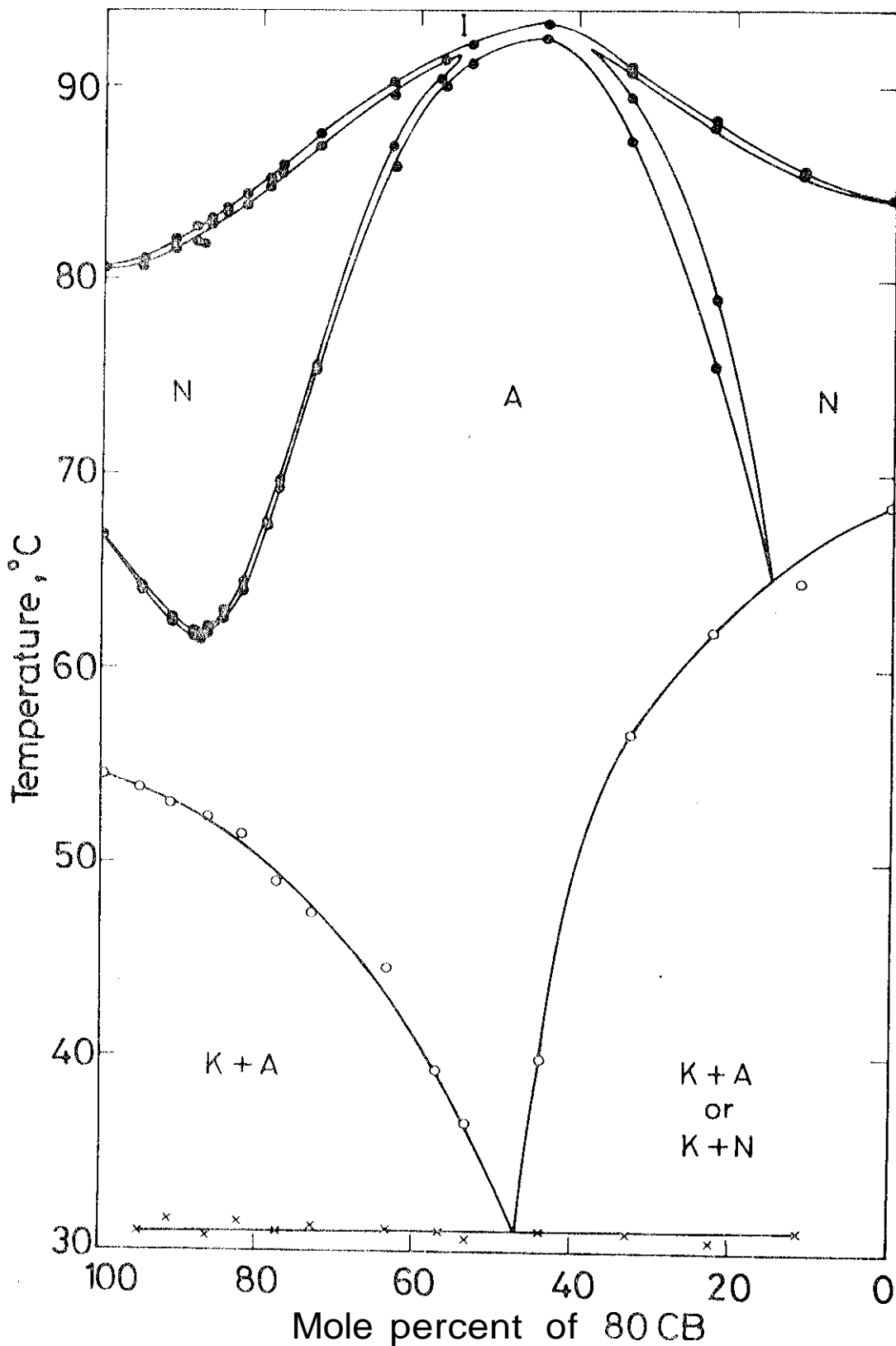


**FIG. 6.4:** Phase diagram of mixtures of NPOOB with OH-EBBA (system I). K stands for the crystalline phase.

defined minimum for a composition rich in the highly polar component ( $\approx 74\%$  of NPOOB). We see that the temperature ranges of coexistence between the A and N, and N and I phases are fairly narrow. For higher percentages of OH-EBBA ( $> 75\%$ ), the mixture exhibits only the N phase.

(ii) Mixtures of 8 OCB and 40.05 (System II): The phase diagram of this system is shown in fig.6.5. 8 OCB has the strongly polar cyano end group while no such strongly polar groups are present in 40.05. 8 OCB exhibits a partially bilayer phase with layer spacing  $\approx 1.4 \mu$ . This system also exhibits a well defined maximum as well as a minimum in the A-N transition boundary. Hence it is worthwhile comparing the phase diagrams of system I and II (figs.6.4 and 6.5). From the two diagrams it is clear that in system II, the tendency to form the induced A phase is much stronger than in system I. In the former, the A phase exists up to very high temperatures and near the peak, it transforms directly to the isotropic phase. On the other hand, the peak in the induced A-N boundary of system I is much less pronounced and lies well below the N-I transition boundary. This means that the interactions responsible for the induction of the A phase are much stronger in system II than in system I.



**BIG.6.5:** Phase diagram of mixtures of 8 OCB with 40.05 (system 11). K stands for the crystalline phase.

This is probably a consequence of the lateral hydroxyl group in OH-EBBA. As a result of this substituent, the average separation between OH-EBBA and NPOOB molecules is likely to be larger than that between 40.05 and 8 OOB molecules. Thus the mutual interaction energy responsible for the induced A phase in system f is smaller than in system if. In system II, the minimum in the A-N boundary occurs for a mixture containing  $\sim 85\%$  of 8 OOB while the maximum is obtained for a composition having  $\sim 50\%$  8 OOB. For very high percentages of 40.05, the mixtures show only the N phase.

We have also calculated the eutectic temperature and composition for both the systems using Schroder-van Laar equations, viz.,

$$\ln P_A = -\frac{\Delta H_A}{R} \left( \frac{1}{T_A} - \frac{1}{T} \right)$$

$$\ln P_B = -\frac{\Delta H_B}{R} \left( \frac{1}{T_B} - \frac{1}{T} \right)$$

where  $\Delta H_A$ ,  $T_A$  and  $\Delta H_B$ ,  $T_B$  are the heats of melting transitions and the melting temperatures of the pure components A and B respectively. T is the melting point of the mixture. Eutectic temperature and composition can be calculated by solving the two equations simultaneously.

The observed and calculated values of eutectic

temperature and composition are listed in table 6.1. We find that in system I, the observed and calculated values of eutectic temperatures are equal while in system PI, the observed value of the eutectic temperature is lower than the calculated value by about 7°. In both the systems, the observed values of eutectic concentrations of the polar compounds (NPOOB and S OCB) are less than the corresponding calculated values. Similar deviations have been found in earlier studies on systems exhibiting induced A phase.<sup>17</sup> This may arise from the formation of charge transfer complexes.

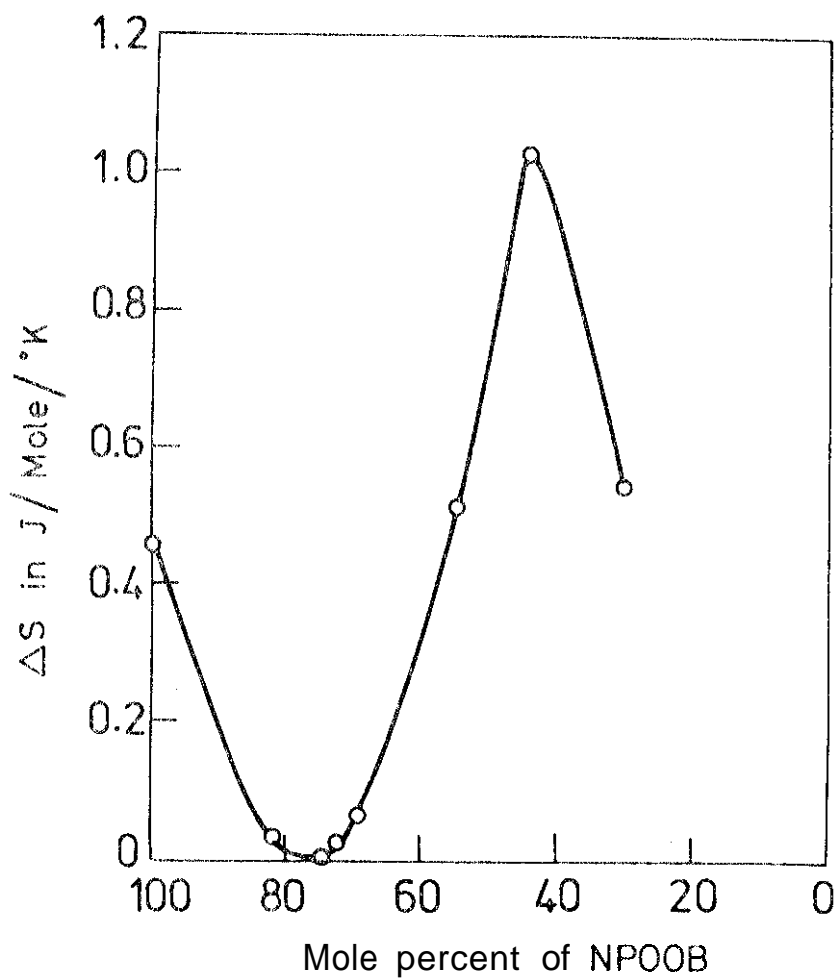
We have calculated the entropy of the A-N transition from DSC curves. The results are presented for system I in fig.6.6. It is interesting to note that the shape of this curve is very similar to that of  $T_{AN}$ , exhibiting a maximum for a composition which also exhibits the maximum in the phase boundary. Further, the A-N transition is almost second order in character for the composition exhibiting the minimum in the phase boundary. A very similar trend is found in system II, the entropy of A-I transition near the maximum being very much larger than the highest value of system I. It is interesting to note that in both the systems, the compositions corresponding to the minima in the A-N boundaries have

Table 6.1

Calculated and observed eutectic temperatures and eutectic compositions for the systems under study

System	Melting points (K)	Heats of melting transition in Joule/Mole	Eutectic Temperatures		Eutectic (Mole %) composition	
			Observed (K)	Calculated (K)	Observed	Calculated
I) KPOOB OH-HBDA	323.7	18450	305	304.8	47.5	65.4
	344.8	23160			52.5	34.6
II) 6 OCB 40.05	327.5	27500	304	311.5	47.0	59.4
	341.5	26580			53.0	40.6





**FIG. 6.6:** The entropy of the A-N transition of system I as a function of composition.

$T_{AN}/T_{NI} \simeq 0.94$ . This ratio is much higher than that required by the McMillan theory,<sup>30</sup> viz.,  $\leq 0.87$  for second order A-N transitions. This once again clearly shows that the interactions responsible for the induced smectic phase in system II are much stronger than those in system I. It is appropriate to mention here that Buka et al<sup>31</sup> have studied the A-N transition enthalpy as a function of composition in mixtures of EBBA and B OCB. The mixture exhibits induced A phase for compositions ranging from  $\sim 20\%$  to  $60\%$  of B OCB. The heat of transition reaches a maximum value for the composition which shows the maximum in the A-N transition boundary.

#### (b) X-ray Studies

We have measured the temperature variations of the layer spacings in the A phase and of the smectic like short range order in the N phase close to  $T_{AN}$  for various compositions of systems I and II. The results are shown in figs. 6.7 and 6.8. Before discussing the results of our experiments, we briefly recall the earlier work by Engelen et al<sup>26</sup> who have measured the layer spacing as a function of composition in mixtures of 4-n-pentylphenyl-4'-n-octyloxybenzoate (B.O.5) and N-p-cyanobenzylidene-p'-n-octyloxyaniline (CBOCA). The layer spacing plotted against composition in this system is shown in fig.6.9.

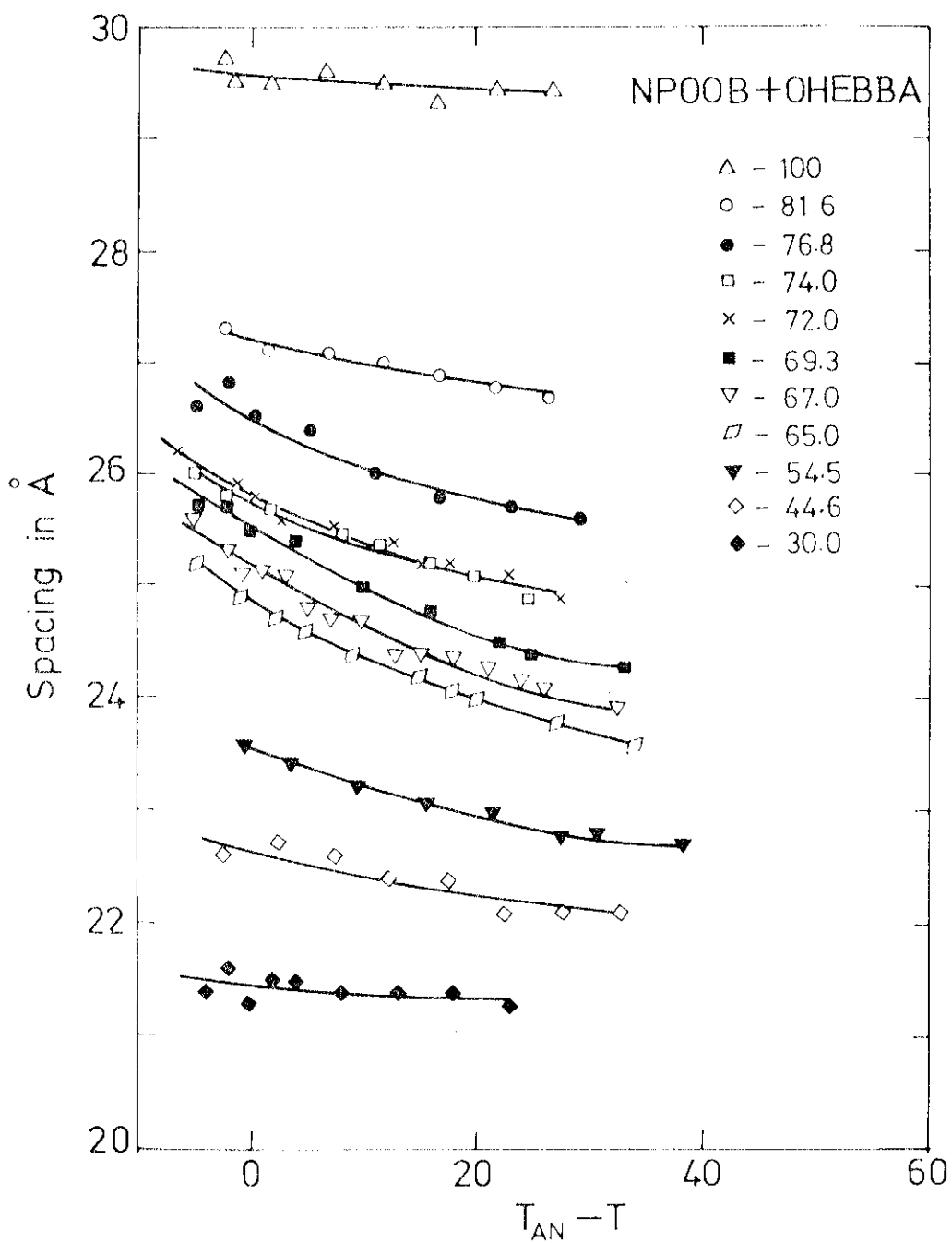


**FIG.6.7:** Layer spacings of mixtures of NPOOB with OH-EBBA as functions of  $(T_{AN} - T)$ . The numbers against different symbols indicate the mole percentage of NPOOB.

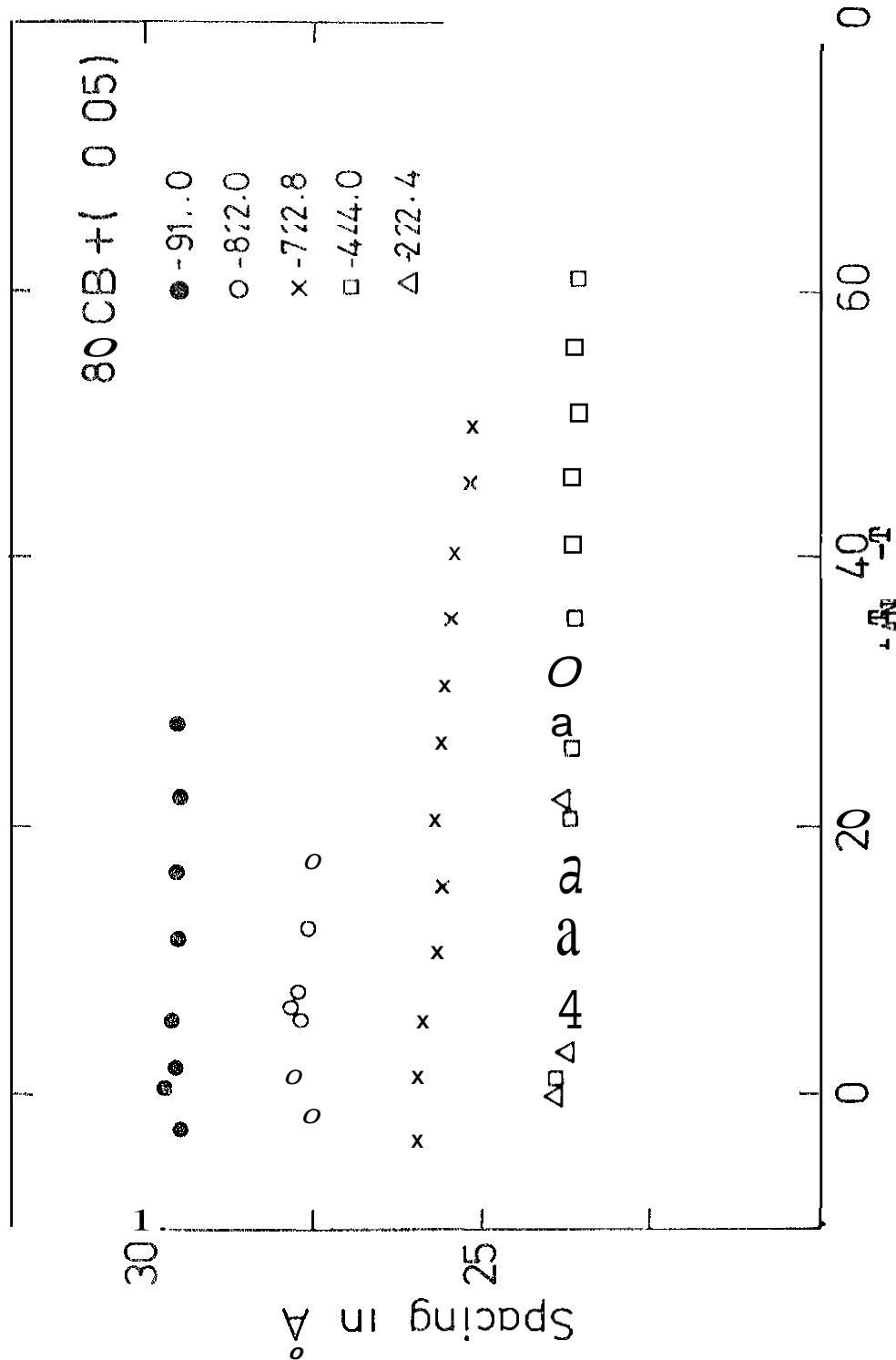
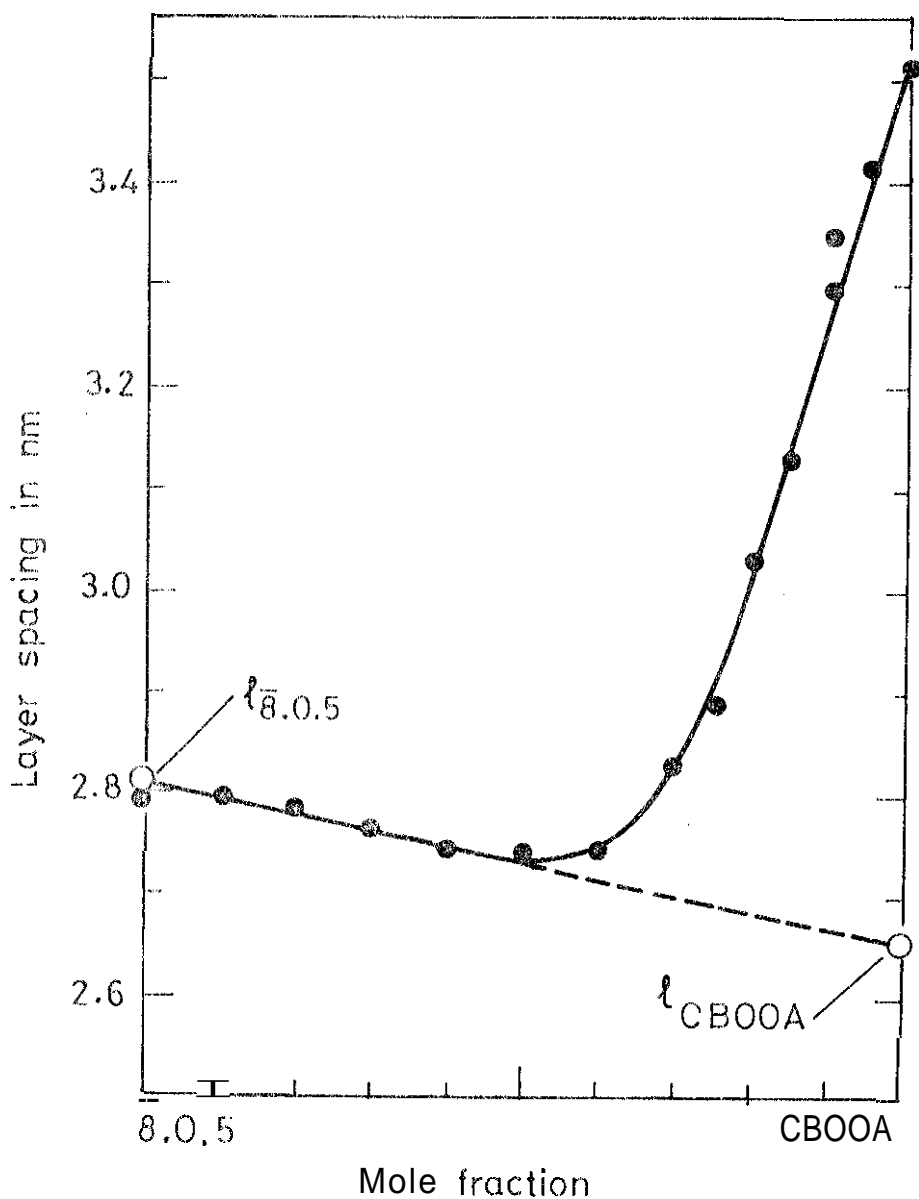
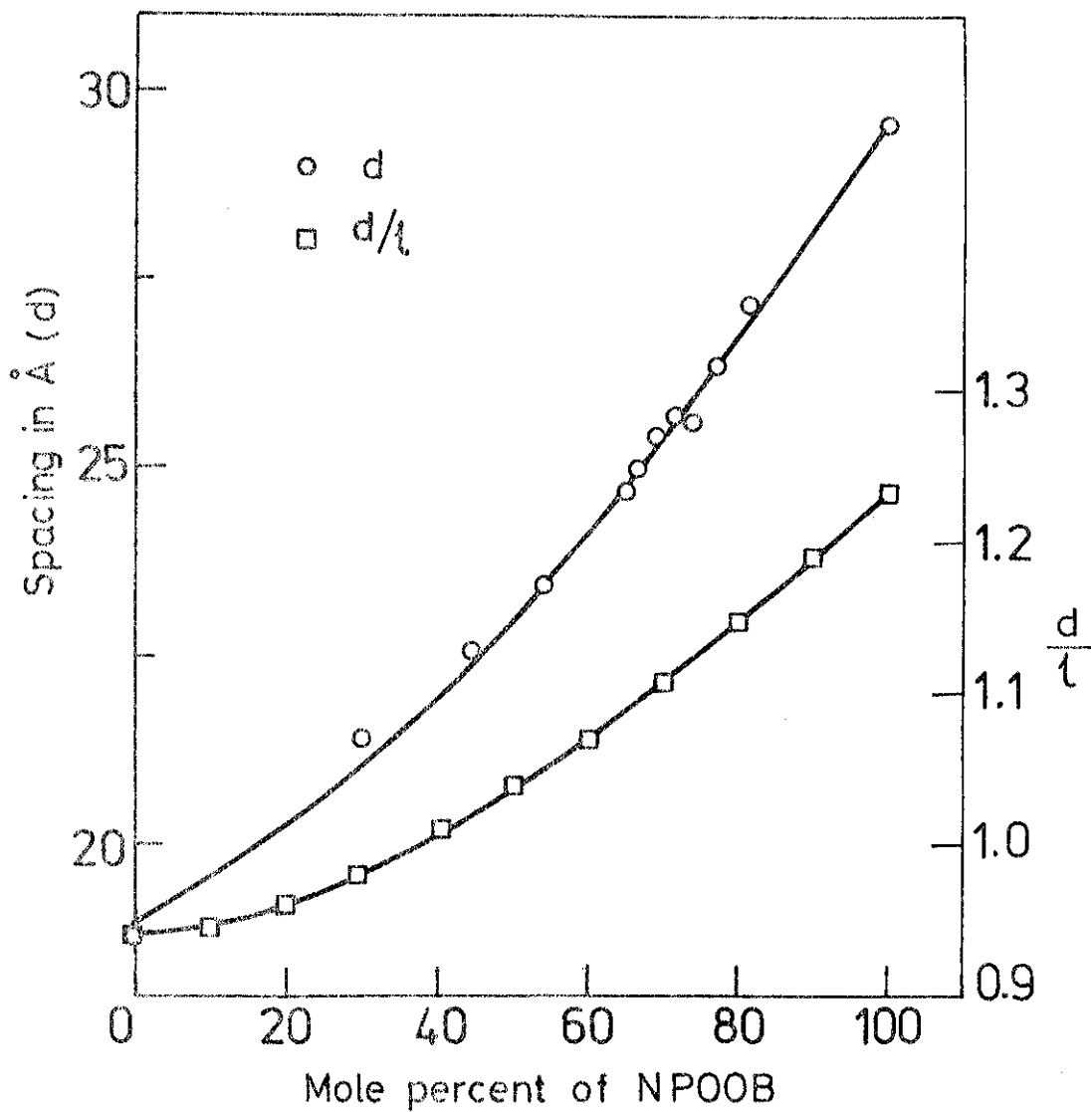


FIG.6.8: Layer spacings of mixtures of 80 CB + ( 0 05) with 40 05 P.S. fractions (TAN - T). The number is against the symbols indicating the percentage of 80 CB.

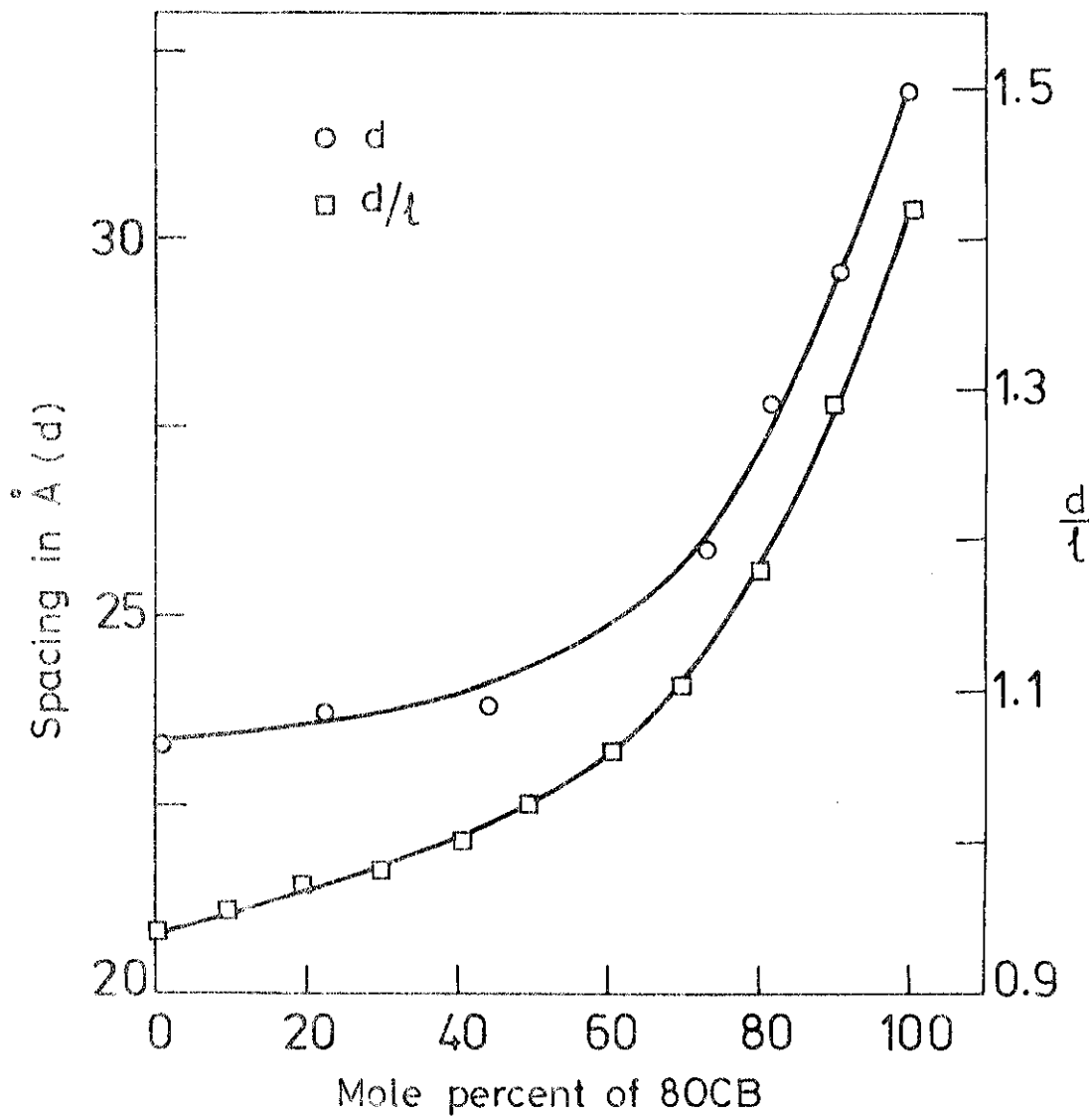
As the percentage of CBOOA in the mixture is increased, the layer thickness decreases almost linearly up to about 50% of CBOOA. When this line is extrapolated to 100% CBOOA, a layer spacing comparable to the molecular length of CBOOA is obtained. But actual measurements show that when the mixture has more than 50% of CBOOA the spacing increases quite sharply approaching the bilayer value of CBOOA as the 0.5 concentration is decreased to zero. It is interesting to notice that the induced smectic-nematic transition curve peaks for a composition with 50% CBOOA. Broadly similar trends can be noticed in the systems studied by us. The variations of layer spacings with composition are shown in figs. 6.10 and 6.11 at a common relative temperature  $T_{AN} - T = 2.5\%$  for the systems I and II respectively. The molecular lengths of the four compounds calculated using Dreiding models are 24.0 Å (NPOOB), 20.2 Å (OH-EBEA), 22.5 Å (8 OCB) and 24.9 Å (4O.05). Using these data, we see that the layer spacings ( $d$ ) for compositions rich in the weakly polar component correspond to average molecular lengths ( $\lambda_{mix}$ ) [calculated using the relation  $\lambda_{mix} = \lambda_1 X_1 + \lambda_2 X_2$  where  $\lambda_1$  and  $\lambda_2$  are the molecular lengths and  $X_1$  and  $X_2$  are the mole fractions of the components]. This means that such compositions consist of only the monolayer species. On the other hand, compositions rich in the strongly polar



**FIG.6.9:** Layer spacing plotted against composition for mixtures of 8.0.5 and CBOOA. The spacings correspond to the temperatures represented by a dashed line in fig.6.2 (Reproduced from ref.26).



**FIG.6.10:** Layer spacing ( $d$ ) and the ratio of the layer spacing to the molecular length ( $d/l$ ) Plotted against composition for mixtures of system I.



**F10.6.11:** Layer spacing ( $d$ ) and the ratio of the layer spacing to the molecular length ( $d/\lambda$ ) plotted against composition for mixtures of system II



component have both monolayer and bilayer species in agreement with results on other systems.<sup>16</sup> Calculations at  $T_{AN} - T = 2.5^\circ$  show that  $(d/\lambda)$  ratio varies smoothly from a value nominally less than one for the weakly polar component to  $\sim 1.23$  in the case of pure NFOOB in system I and to  $\sim 1.42$  in the case of S OOB in system II. The  $d$  values of NFOOB and S OOB agree with earlier measurements.<sup>32,24</sup>

We did not find any evidence of  $S_A - S_A$  transition in our X-ray studies on the two systems. The well defined minima in the phase diagrams indicate that  $A_2$  and  $A_1$  (i.e., induced smectic) phases may not be structurally compatible (in some cases it is found that the  $A_2$  phase and the induced A phase are immiscible<sup>26</sup>). However, the coexistence of both We bimolecular and monomolecular species for compositions close to the minima, as indicated by a continuous variation in lattice parameter, smears out any possible sharp  $A_2 - A_1$  transition.

We notice from fig.6.7 that the thermal expansion coefficient of the layer spacing of system I increases as we approach a composition corresponding to the minimum in the A-N boundary from either side. This is brought out clearly in fig.6.12. Further, the expansion coefficient increases with increase of temperature for any given

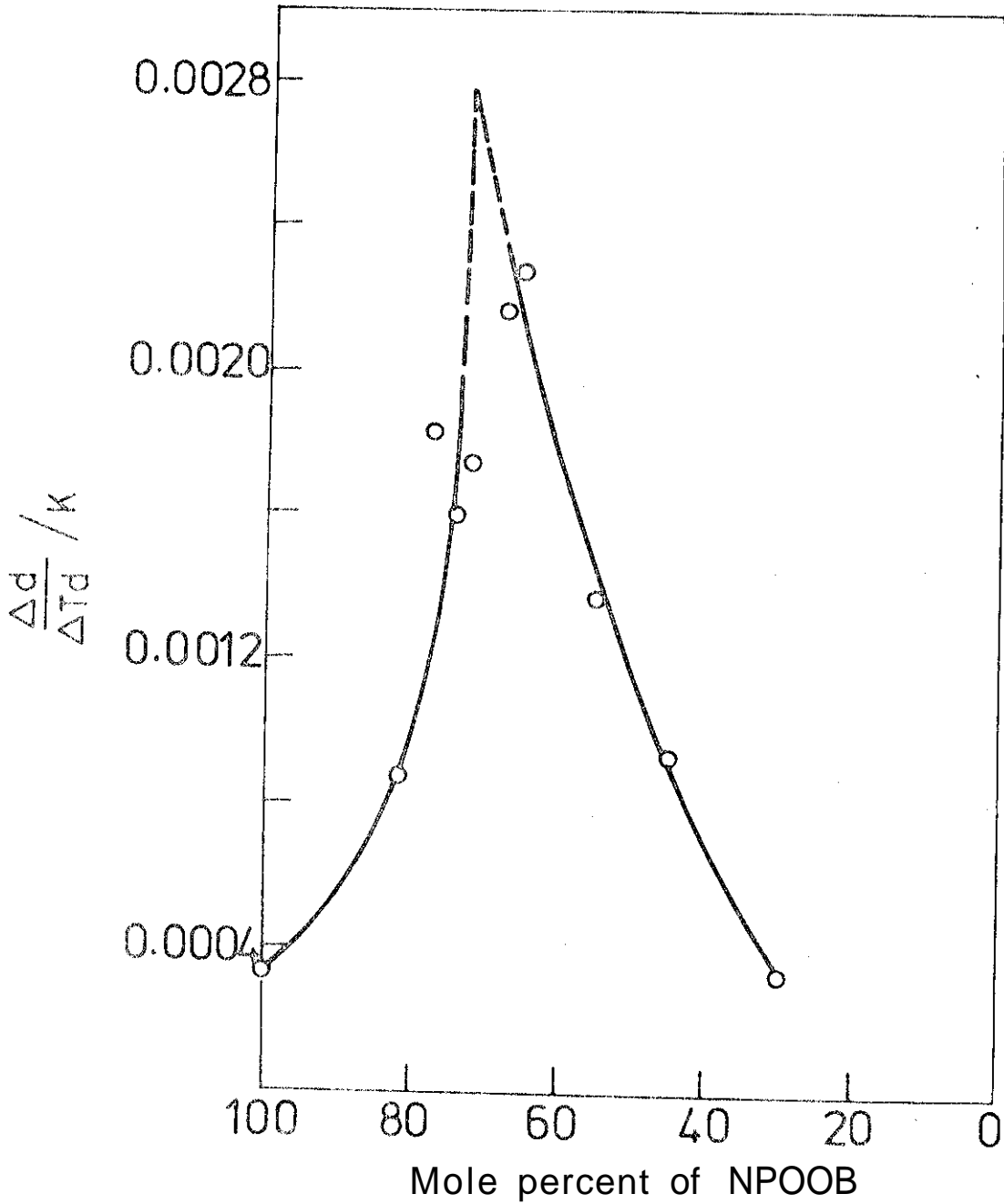


FIG.6.12: The thermal expansion coefficient of the layer spacings of mixtures of NPOOB with OH-EBBA at  $T_{AN} - T = 2.5^\circ$ .

composition in this region. On the other hand, such a trend is not very conspicuous in system II. We attribute this difference in behaviour between the two systems to the large difference in the strengths of the intermolecular interactions between the components in the two cases. As discussed earlier, the interaction between the strongly polar and weakly polar molecules is relatively weak in system I, mainly because of the lateral hydroxyl group of OH-EBBA molecules, and perhaps only slightly higher than the interaction energy which gives rise to antiparallel correlations between two neighbouring NPOOB molecules. Consequently, as the temperature is raised, firstly the thermal expansion coefficient of layer spacing can be considerable as we discussed in chapter III in the case of compounds with bulky lateral substituents, and further, the strongly polar-weakly polar pairs can easily break up allowing NPOOB molecules to form more antiparallel pairs and thus the thermal expansion coefficient can be very large. It can also be noted that for compositions near the minimum, there are three NPOOB molecules for every OH-EBBA molecule. Further, for these compositions  $A_2$  and  $A_1$  structures coexist and the A-N transition has a second order character. As a result, the thermal expansion coefficient attains large value for composition close to the minimum in the phase boundary.

(c) Static dielectric constants

Temperature variations of the principal dielectric constants ( $\epsilon_{11}$  and  $\epsilon_{\perp}$ ) in the A and N phases and  $\epsilon_{is}$  in the isotropic phase were measured for various systems and are shown in figs. 6.13 - 6.22.

In the case of pure NPOOB, both  $\epsilon_{11}$  and  $\epsilon_{\perp}$  show a decrease as the sample is cooled across  $T_{AN}$  (fig. 6.13). Our values are in broad agreement with earlier measurements on this compound.<sup>33,34</sup> NPOOB has a weakly first order A-N transition (fig. 6.6) and the increase of  $\epsilon_{11}$  and decrease of  $\epsilon_{\perp}$  as the sample is cooled in the A phase probably means that the anti-parallel correlations do not vary much with temperature in the A phase and the variations are essentially determined by that of the orientational order. The  $\bar{\epsilon} = \frac{\epsilon_{11} + 2\epsilon_{\perp}}{3}$  value increases with temperature in the N phase, indicating a corresponding decrease of anti-parallel correlations (as discussed in chapters III and IV). As the temperature is raised in the isotropic phase,  $\epsilon_{is}$  exhibits a broad maximum, again due to a decrease in antiparallel correlations at higher temperatures. In the mixture containing 90.2% NPOOB, as the sample is cooled,  $\epsilon_{11}$  decreases slightly across  $T_{AN}$  (fig. 6.14), attains a broad minimum and then increases slightly in the lower temperature range of the A phase.

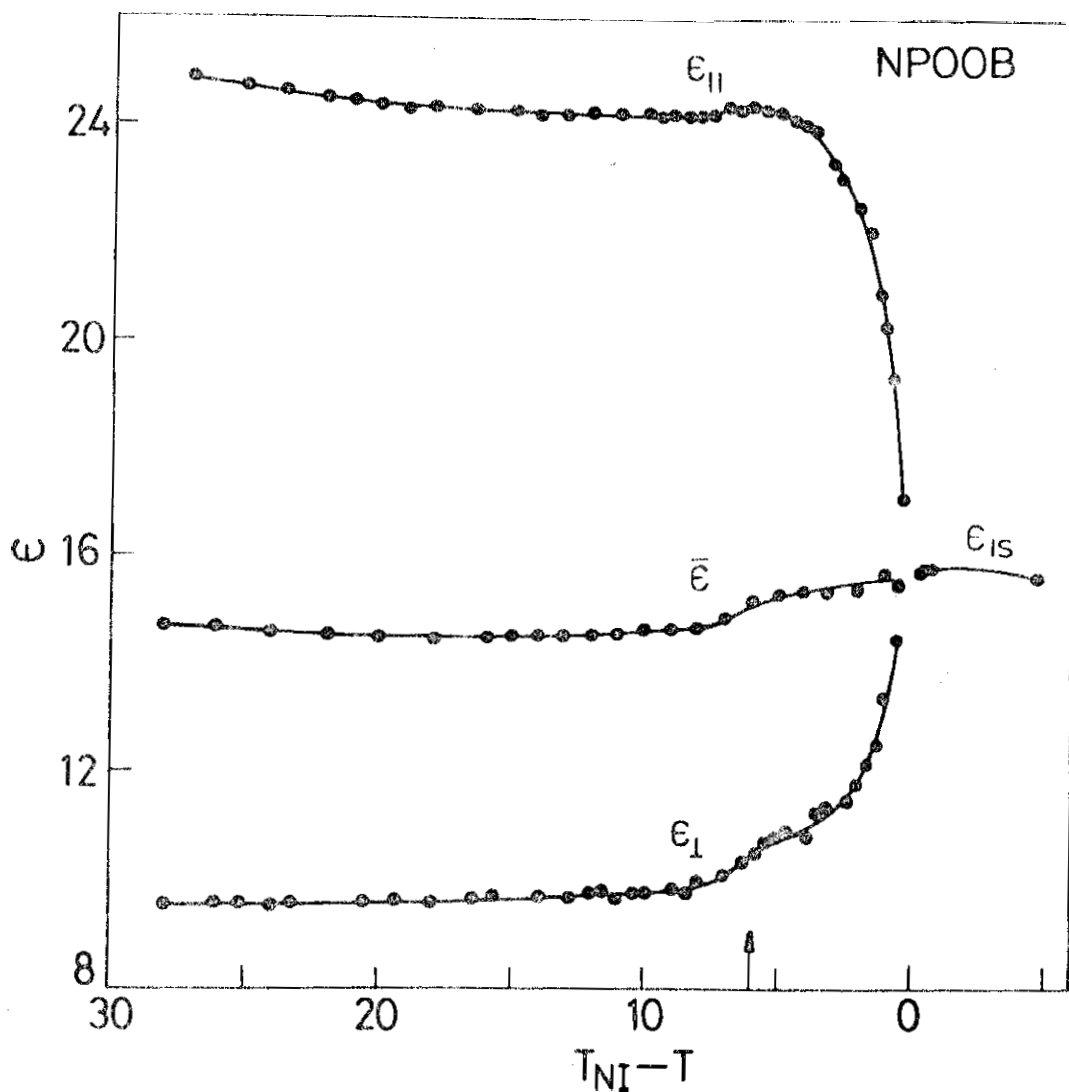


**FIG.6.13:** Low frequency dielectric constants (measured at 1592 Hz) of NPOOB as functions of relative temperature. The vertical arrow on the temperature axis indicates  $T_{AN}$ .

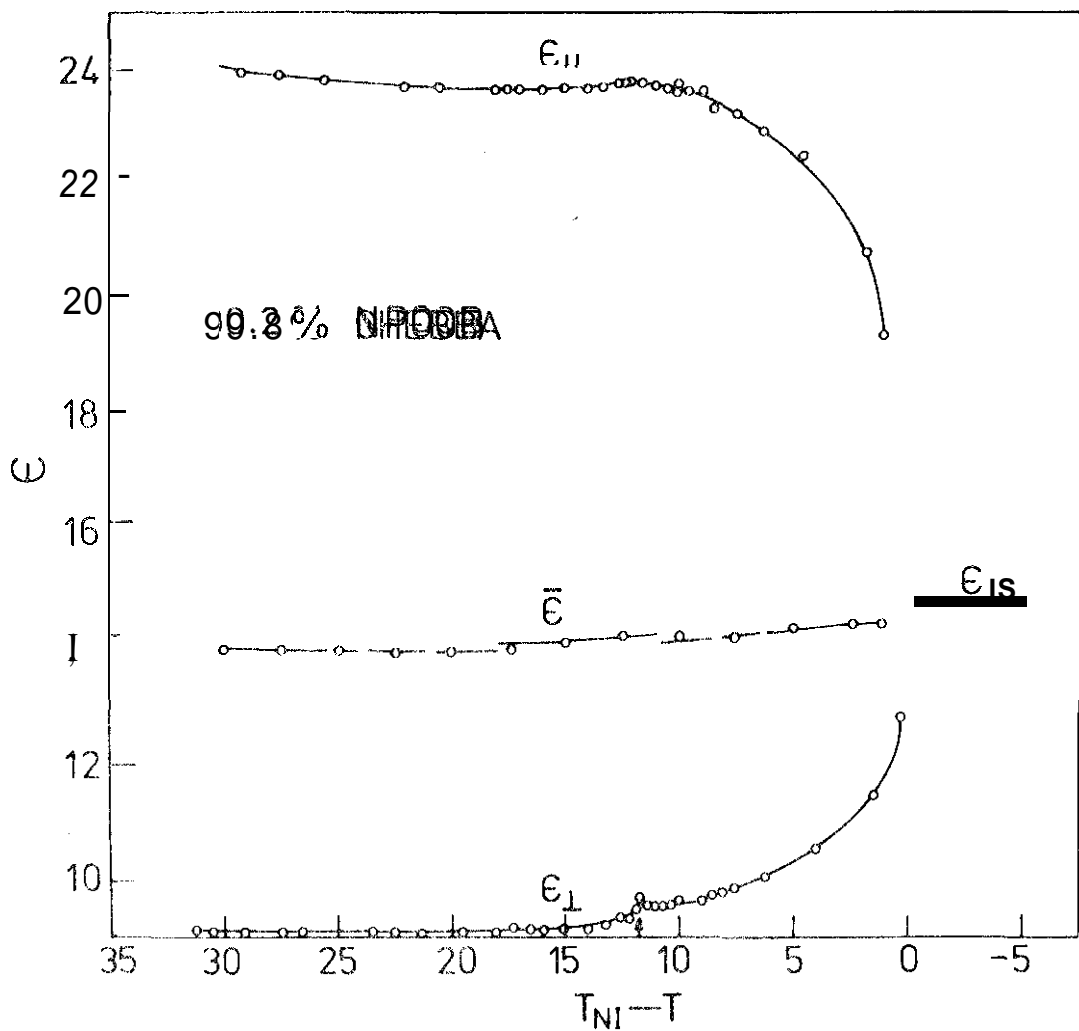


**FIG.6.14 :** Low frequency dielectric constants (measured at 1592 Hz) of a mixture of 90.2 mole per cent of RPOOB with 9.8 mole per cent of CH-EBBA as functions of relative temperature. The vertical arrow indicates  $T_{AN}$ .

$\epsilon_{\perp}$  remains practically constant in the A phase.  $\bar{\epsilon}$  again increases with temperature in the N phase which is due to a decrease in antiparallel correlations. Similar trends are observed in the temperature variation of  $\epsilon_{\perp}$  in the mixtures containing 76.8% NPOOB (fig.6.15), 74% NPOOB (corresponding to the minimum in the A-N boundary)(fig.6.16), 72% NPOOB (fig.6.17) and 67% NPOOB (fig.6.18). But it is interesting to note that for these mixtures  $\epsilon_{\perp}$  increases with decrease of temperature in the A phase. This can be easily understood in terms of the increase in the number of strongly polar-weakly polar molecular pairs at the expense of Use antiparallel strongly polar molecular pairs. Assuming that the charge-transfer complexes are forming, it is clear that the transverse polarisability and hence  $\epsilon_{\perp}$  should increase. As can be seen from the diagrams, the degree of enhancement in  $\epsilon_{\perp}$  value increases with increasing concentration of OH-EBBA. This again shows that more number of complexes are formed with increasing number of OH-EBBA molecules. For these compositions  $\bar{\epsilon}$  value increases slightly as the temperature is lowered in the N and A phases.  $\bar{\epsilon}$  decreases very slightly as the temperature is raised in We isotropic phase. The cusp-like peak observed in  $\epsilon_{\perp}$  near  $T_{AN}$  arises from the strong tendency of the director to orient homeotropically in the A phase

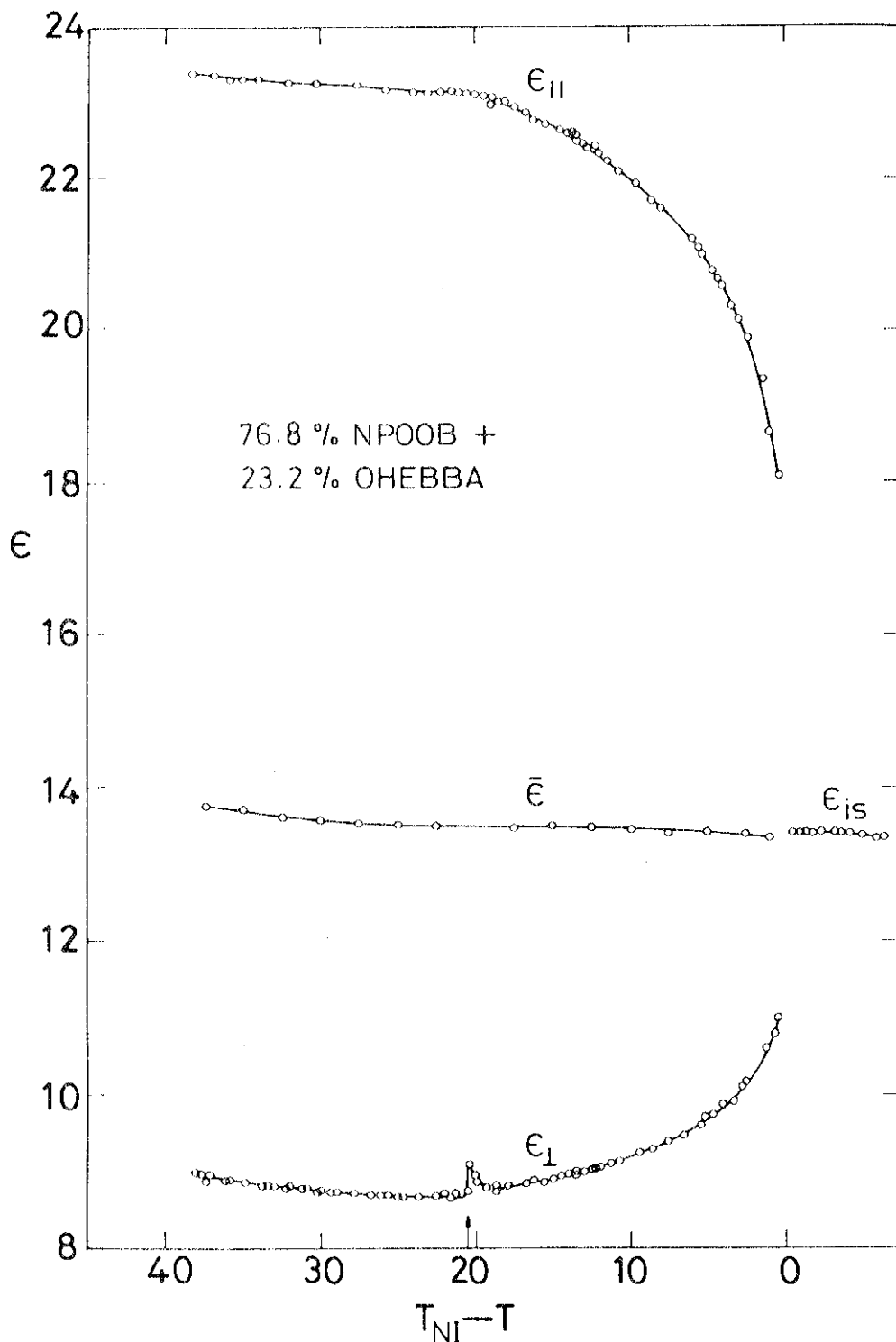


**FIG.6.15:** Low frequency dielectric constants (measured at 1592 Hz) of a mixture of 76.8 mole % of NPOOB with 23.2 mole % of OH-EBBA as functions of relative temperature. The vertical arrow indicates  $T_{AN}$ .



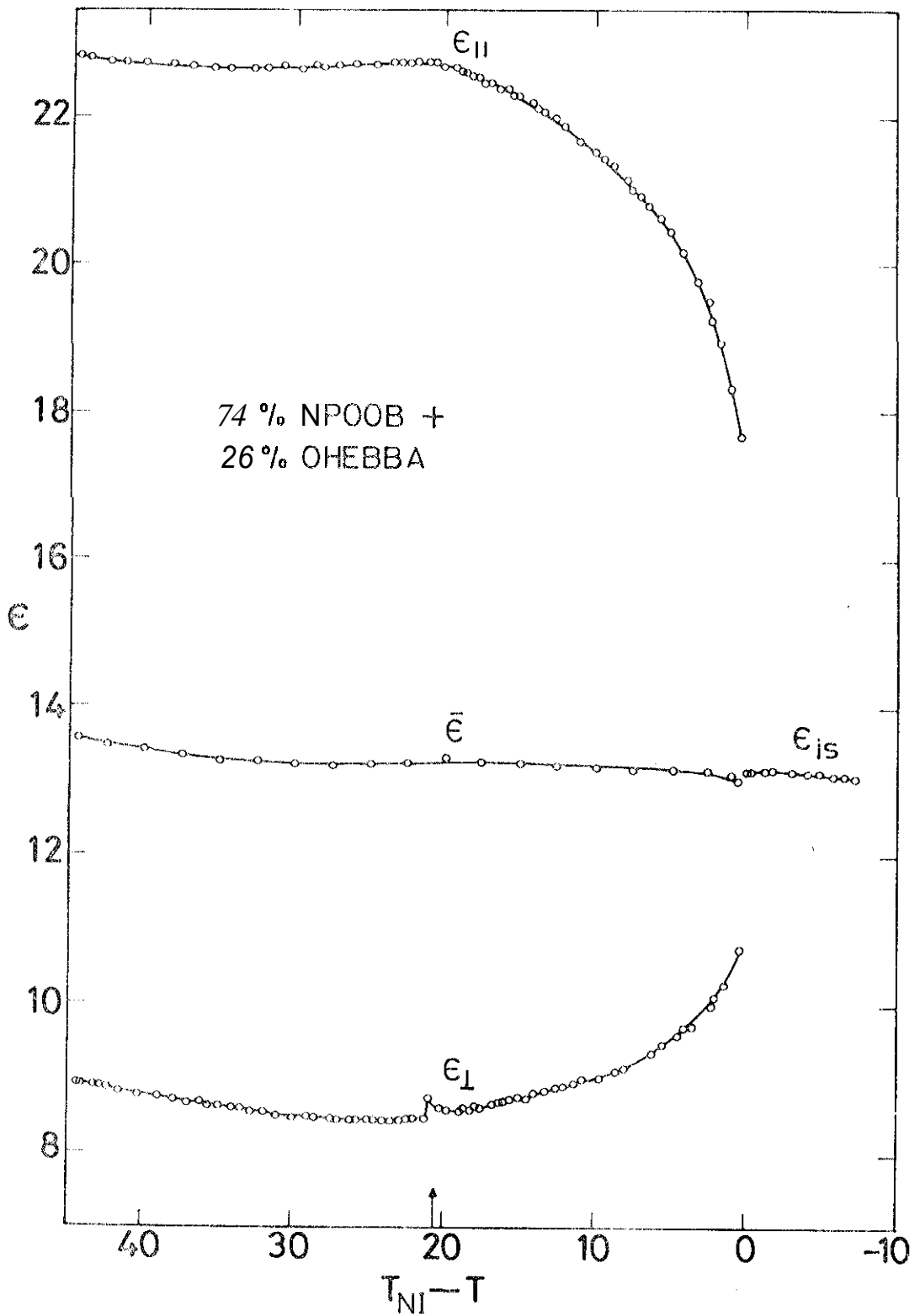
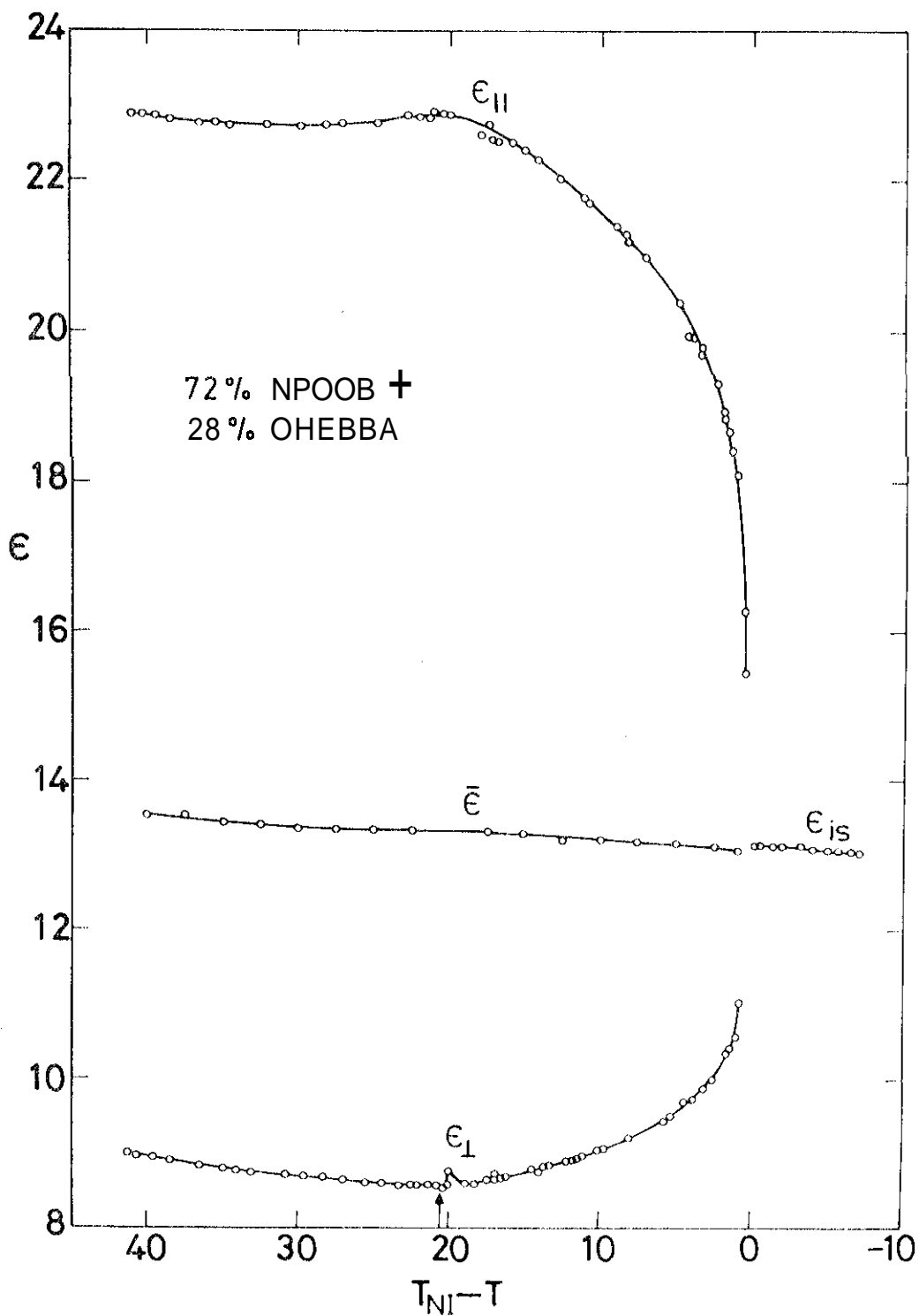


FIG. 6.16: Low frequency dielectric constants (measured at 1592 Hz) of a mixture of 74 mole per cent of MPOOB with 26 mole per cent of OH-EBBA as functions of relative temperature., The vertical arrow indicates  $T_{AN}$ .



**FIG. 6.17:** Low frequency dielectric constants (measured at 1592 Hz) of a mixture of 72 mole % of NPOOB with 28 mole % of OH-EBBA as functions of relative temperature. The vertical arrow indicates  $T_{AN}$ .

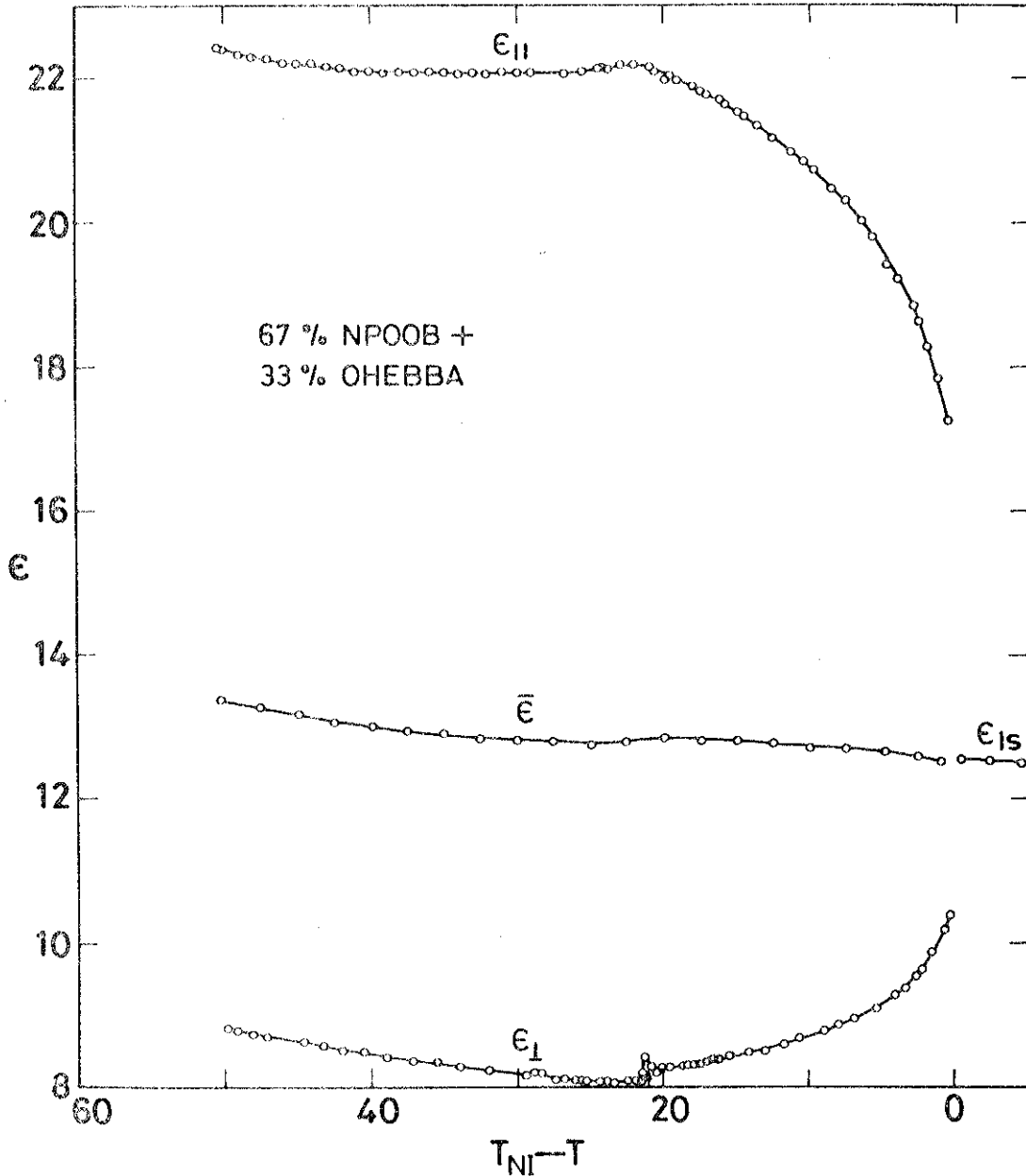
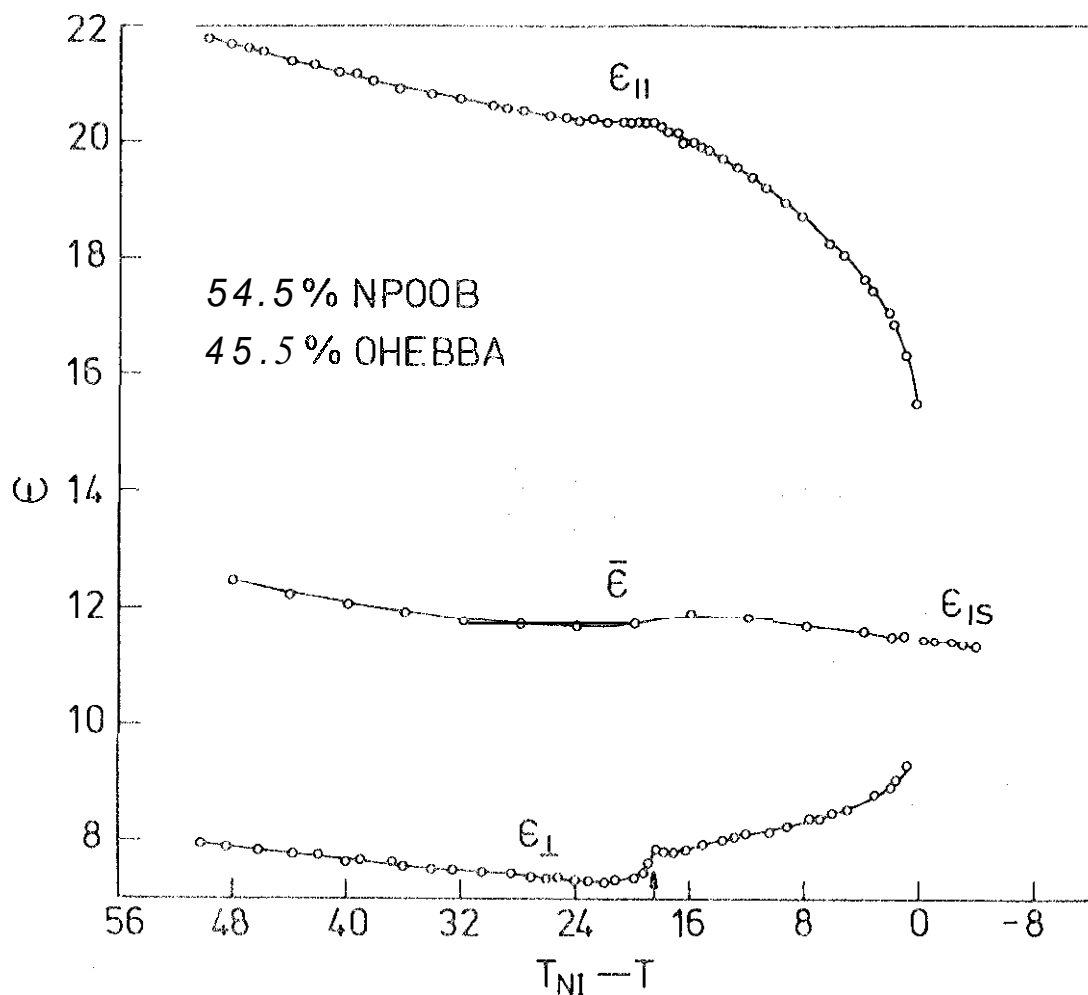


FIG.6.18: Low frequency dielectric constants (measured at 1592 Hz) of a mixture of 67 mole % of NPOOB with 33 mole % of OH-EBBA as functions of relative temperature. The vertical arrow indicates  $T_{AN}$ .

for these compositions<sup>35</sup> in the neighbourhood of  $T_{AN}$ . In all the mixtures discussed so far  $\bar{\epsilon}$  shows a positive jump at  $T_{NI}$ . However, the magnitude of the jump decreases with increase of OH-EBBA component. Such jumps have been observed in several earlier studies<sup>36,37</sup> which are now well understood (as discussed in chapter IV) as arising from a decrease in the number of antiparallel pairs. With the result that the effective contribution at the dipolar groups of the polar molecules to the dielectric constant is enhanced.

The results for a mixture containing 54.5% NPOOB which is a composition near the maximum in the A-N boundary is shown in fig.6.19. As the temperature is decreased, a very small decrease in  $\epsilon_{\parallel}$  value is observed near  $T_{AN}$ . But  $\epsilon_{\perp}$  shows a larger jump near  $T_{AN}$ . Both  $\epsilon_{\parallel}$  and  $\epsilon_{\perp}$  increase with decrease of temperature in the A phase. These results are more pronounced in a mixture containing 44.6% NPOOB which is even closer to the maximum (fig.6.20). For this composition we see quite a strong reduction in both  $\epsilon_{\parallel}$  and  $\epsilon_{\perp}$  as the sample is cooled across  $T_{AN}$ . This may be attributed to the fact that  $\Delta H$  heat of A-N transition is quite large for this composition (fig.6.6) and the orientational order parameter can be expected to jump to a higher value in the A phase.<sup>30</sup> The decrease in  $\epsilon_{\parallel}$



**FIG.6.19:** Low frequency dielectric constants (measured at 1592 Hz) of a mixture of 54.5 mole % of NPOOB with 45.5 mole percent of OH-EBBA as functions of relative temperature. The vertical arrow indicates  $T_{AN}$ .

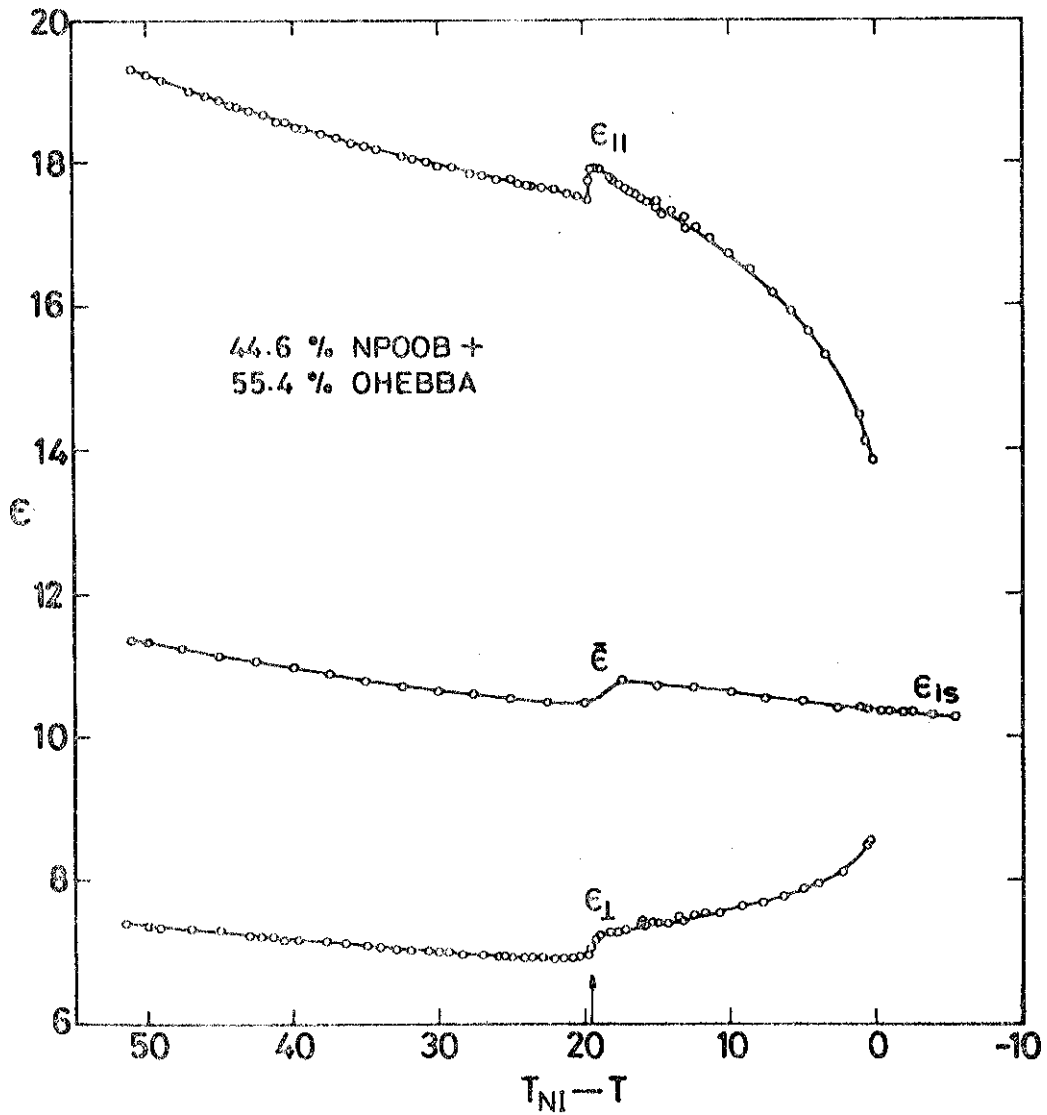
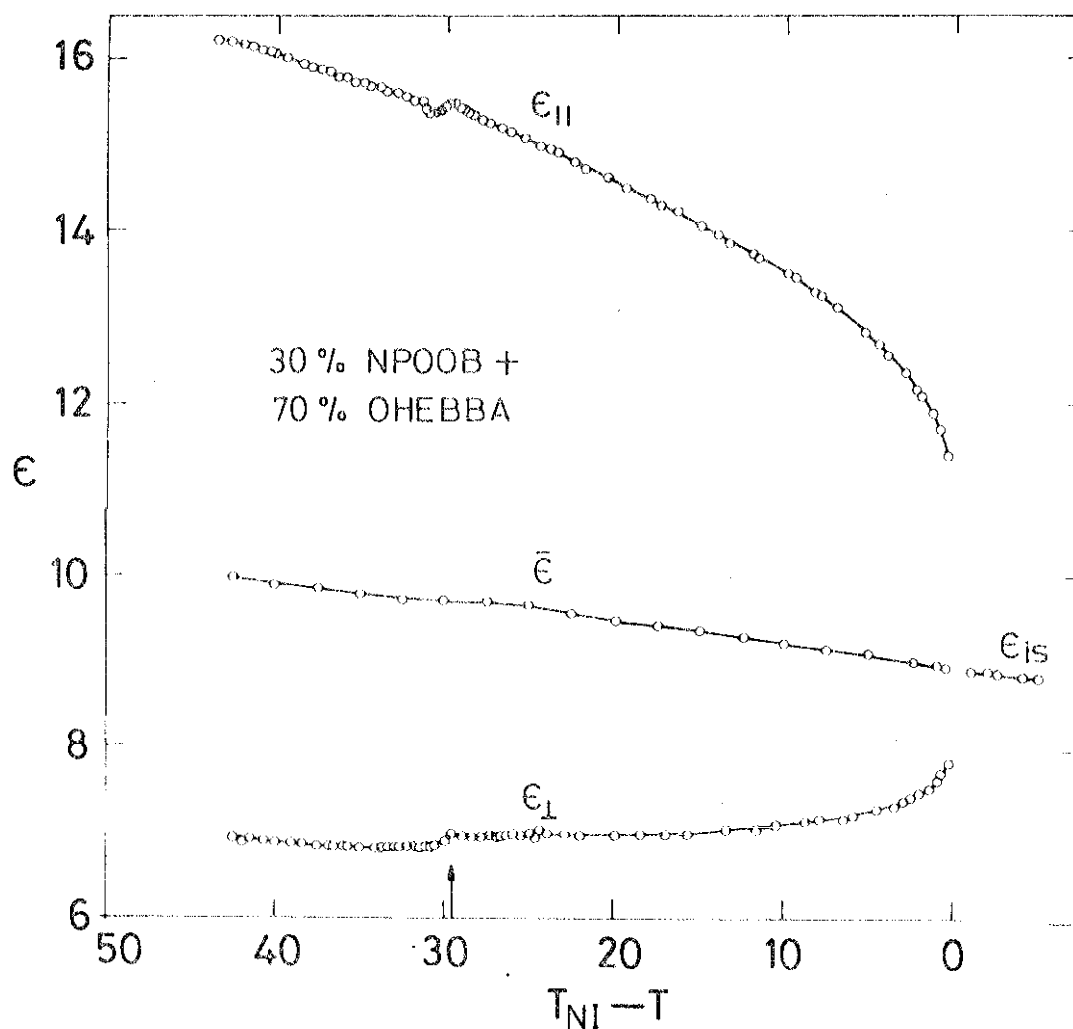


FIG.6.20: Low frequency dielectric constants (measured at 1592 Hz) of a mixture of 44.6 mole % of NPOOB with 55.4 mole % of OH-EBBA as functions of relative temperature. The vertical arrow indicates  $T_{AN}$ .

probably arises partly from an increase in the anti-parallel correlations of the NFOOB molecular pairs and partly due to the tendency of the director to prefer a homogeneous alignment in this composition range. However, the strongly polar-weakly polar molecular pairs should be *very* large for these compositions which are close to the maximum in the phase boundary, and the permanent dipole moments of the individual molecules belonging to such pairs fully contribute to  $\epsilon_{\parallel}$ , unlike in the case of pairs of antiparallel NFOOB molecules in which there is a partial compensation of the dipole moment. Further, the charge transfer complex pairs increase *with* decrease of temperature. Thus  $\epsilon_{\parallel}$  increases substantially as the temperature is lowered in the A phase.  $\epsilon_{\perp}$  also increases with decrease of temperature as already discussed for the compositions having a higher concentration of NFOOB. For these compositions (close to the maximum in the A-N boundary), no jump is observed in  $\bar{\epsilon}$  value at  $T_{NI}$ . This is due to the relatively small number of antiparallel pairs in such compositions.

With further decrease of NFOOB concentration (30% NFOOB, fig.6.21), the effects observed for the 44.611 NFOOB mixture get less pronounced and understandably the increase of  $\epsilon_{\perp}$  with lowering of temperature becomes weak.



**FIG.6.21:** Low frequency dielectric constants (measured at 1592 Hz) of a mixture of 30 mole % of NPOOB with 70 mole % of OH-EBBA as functions of relative temperature. The vertical arrow indicates  $T_{AN}$ .



The principal dielectric constants of OH-EBBA are shown in fig.6.22. As can be seen from the figure, OH-EBBA itself has a negative dielectric anisotropy, as the net dipole moment of the molecule makes a large angle with the long axis.  $\epsilon_{\perp}$  increases and  $\epsilon_{\parallel}$  decreases with decrease of temperature.  $\bar{\epsilon}$  and  $\epsilon_{10}$  decrease almost linearly with increase of temperature. All these trends can be understood in terms of the Maier and Meier's theory (see chapter IV) as applied to a compound with negative  $\Delta\epsilon$ .

The dielectric anisotropies of all the mixtures that we have studied are collected in fig.6.23. It is quite clear that the temperature variation of  $\Delta\epsilon$  in the A phase is quite different for compositions close to the minimum in the AN boundary compared to those close to the maximum.

In compositions close to the minimum, the A-N transition is weak and hence the smectic order increases, as the temperature is lowered in the A phase with a corresponding increase in the dipolar correlation factor in the layered structure which tends to decrease  $\epsilon_{\parallel}$ . This would compensate for any increase in  $\epsilon_{\parallel}$  due to stronger charge transfer interactions and hence  $\epsilon_{\parallel}$  does not increase much at lower temperatures. Hence  $\Delta\epsilon$

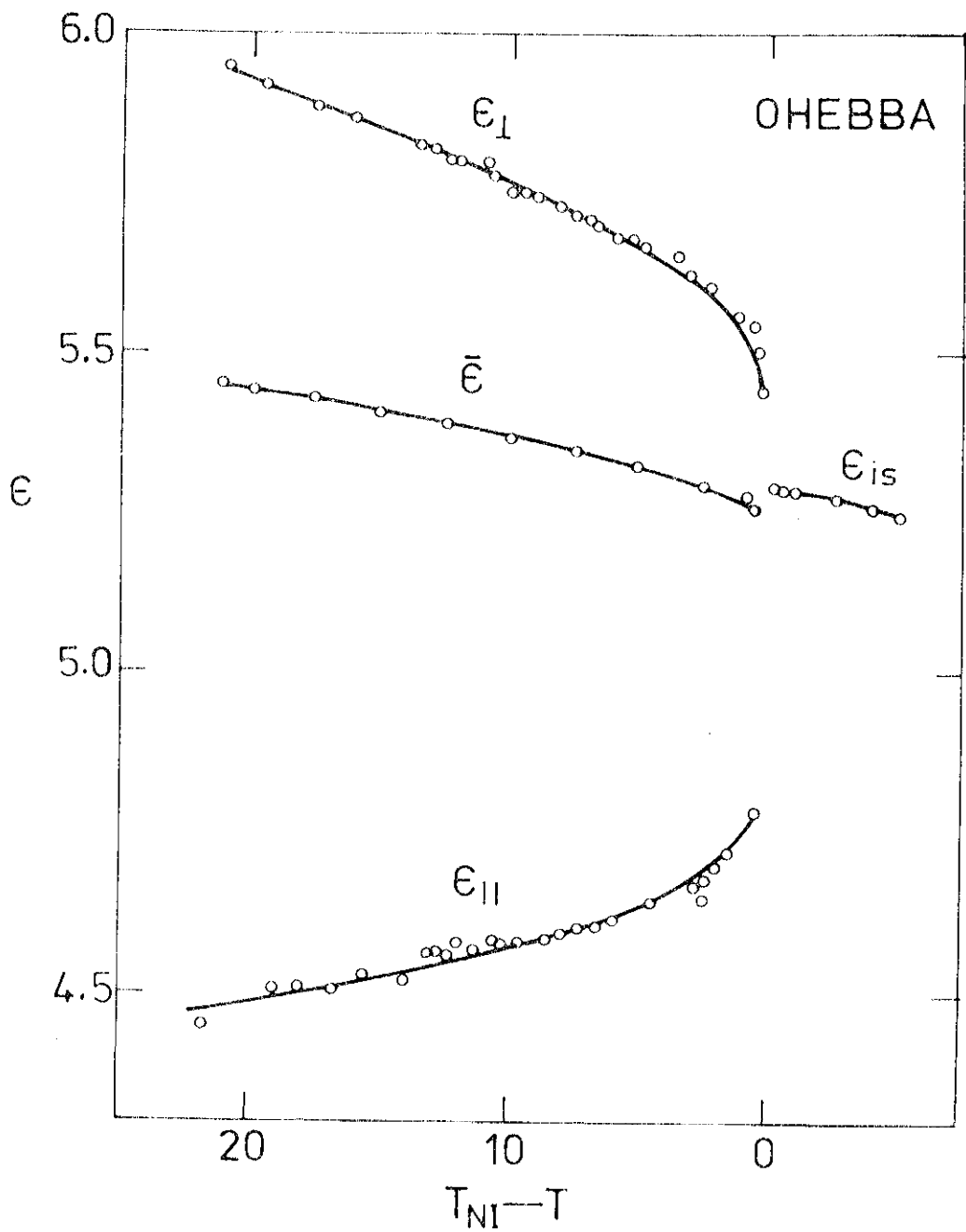


**FIG.6.22:** Low frequency dielectric constants (measured at 1592 Hz) of OH-EBBA as functions of relative temperature.

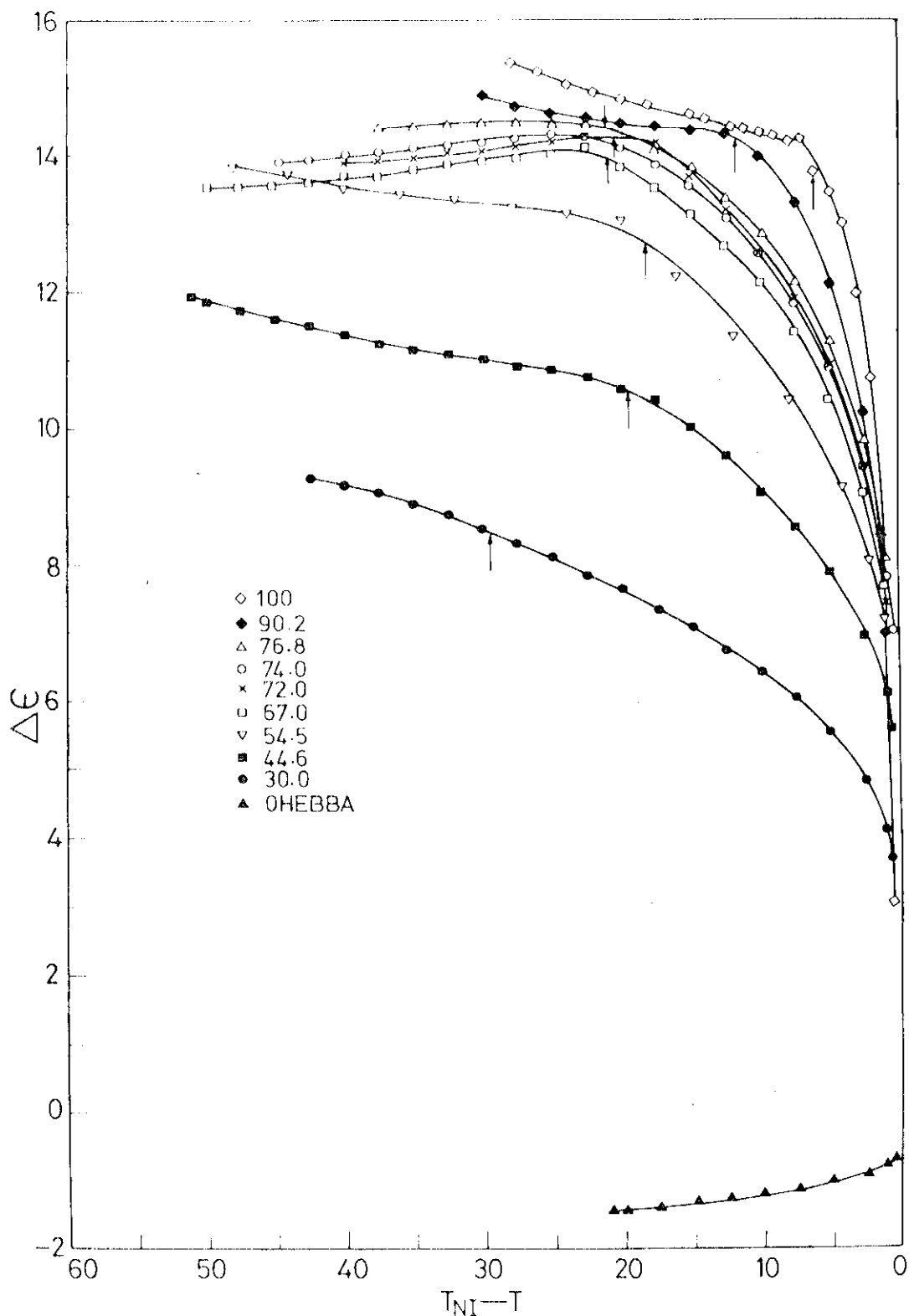


**FIG.6.23:** Dielectric anisotropies of mixtures of NPOOB with OH-EBBA as functions of relative temperature. The numbers against different symbols indicate mole percentages of NPOOB and the arrows indicate  $T_{AN}$ .

decreases at lower temperatures.

Near the maximum in the phase boundary (54.5% NPOOB or 44.6% NPOOB), the A-N transition has strong first order characteristics, and the increase in the antiparallel dipolar correlation factors would lead to a decrease with a jump of  $\epsilon_{\perp}$  (fig.6.19 & fig.6.20) at the A-N transitions. The jump in the orientational order parameter would lead to a decrease in  $\epsilon_{\perp}$  also at this point. But as the smectic order is already strong at  $T_{AN}$ , it does not vary much with a further lowering of temperature. The increase in the number of charge transfer pairs would lead to an increase of  $\epsilon_{\perp}$  due to the more effective contribution of  $\text{NO}_2$  dipoles in such pairs. This effect appears to be stronger than the increase of  $\epsilon_{\perp}$  due to the increase in the transverse polarizability of the charge transfer pairs and  $\Delta\epsilon$  actually increases with decrease of temperature. We may also point out two unusual features: (I) the mixture with 74% NPOOB has a lower value of  $\Delta\epsilon$  than that of the mixture with 72% NPOOB in the N phase close to  $T_{AN}$ ; (ii) because of the opposite variation of  $\Delta\epsilon$  with temperature in the A phase of the mixtures with 54.5% NPOOB compared to mixtures with higher percentages of NPOOB, at sufficiently low temperatures, the former has higher

$\Delta\epsilon$  values than many mixtures of the latter type.

It is also interesting to compare the measured values of  $\Delta\epsilon$  and  $\bar{\epsilon}$  of the mixtures with the corresponding numbers calculated on the basis of an additive law of the type  $\Delta\epsilon_{\text{mix}} = P_1 \Delta\epsilon_1 + P_2 \Delta\epsilon_2$ , where  $P_1$  is the mole fraction of the first component, etc. The results are shown in table 6.2.

It is clear that  $\Delta\epsilon_{\text{meas}}/\Delta\epsilon_{\text{calc}}$  is larger than unity (in agreement with some earlier observations<sup>13</sup>) and increases with increasing percentage of OH-EBBA. This is mainly because the probability of breaking up of antiparallel associations between NPOOB molecules increases with increasing percentage of OH-EBBA molecules. Consequently, the  $\text{NO}_2$  group can more effectively contribute to  $\epsilon_{\parallel}$ . As can be easily seen from the diagrams 6.13- 6.22,  $\epsilon_{\parallel}$  of mixtures is much higher than what an additive law would have given (table 6.3). The  $\epsilon_{\perp}$  value does not change very much between NPOOB and OH-EBBA and hence does not contribute much to the deviation of the above ratio from unity.  $\bar{\epsilon}_{\text{meas}}/\bar{\epsilon}_{\text{calc}}$  shows values which are greater than one by  $\sim 10-20\%$ .

We have also measured the temperature variations of static dielectric constants for a mixture of 63.5% NPOOB

Table 6.2

Comparison of the measured and calculated values of  $\Delta\epsilon$   
and  $\bar{\epsilon}$  of various mixtures at  $T_{NI} - T = 20^\circ$

Mole percent of NPOOB	Calculated value		Measured value		Ratio of measured to calculated values	
	$\Delta\epsilon$	$\bar{\epsilon}$	$\Delta\epsilon$	$\bar{\epsilon}$	R( $\Delta\epsilon$ )	R( $\bar{\epsilon}$ )
100.0	-	-	14.80	14.41	-	-
90.2	13.22	13.52	14.45	13.90	1.09	1.03
76.8	11.03	12.32	14.30	13.50	1.30	1.09
74.0	10.58	12.07	14.10	13.25	1.33	1.10
72.0	10.25	11.89	14.20	13.35	1.39	1.12
67.0	9.44	11.44	13.80	12.80	1.46	1.12
54.5	7.41	10.32	12.85	11.70	1.73	1.13
44.6	5.80	9.44	10.55	10.50	1.82	1.11
30.0	3.43	8.13	7.60	9.50	2.22	1.17
OH-EBBA	-	-	-1.45	5.44	-	-

Table 6.3

Comparison of calculated and observed values of  $\epsilon_{II}$  at  $T_{NI} - T = 5^\circ$  for various mixtures of System I

Mixture Mole % of NPOOB	Values of $\epsilon_{II}$	
	Observed	Calculated $(\epsilon_{II})_{mix} = P_1(\epsilon_{II})_1 + P_2(\epsilon_{II})_2$
100	24.2	-
90.2	22.4	22.3
76.8	20.9	19.7
74.0	20.4	19.1
72.0	20.4	18.7
67.0	19.6	17.7
54.5	18.0	15.3
44.6	15.7	13.4
30	12.8	10.5
OH-EBBA	4.64	-

and 36.5% 40.05 of system II which is close to the maximum of the A-N transition boundary. The results are shown in fig.6.24 and are basically similar to those for a similar composition of system I.

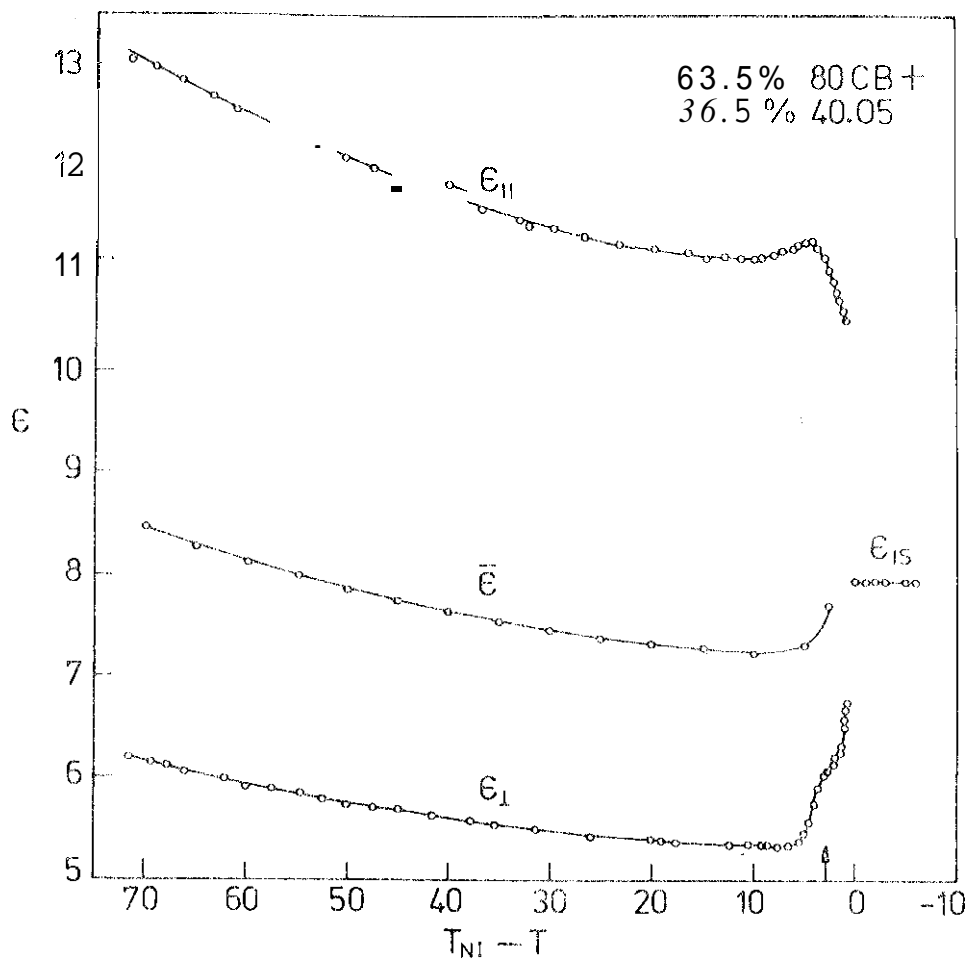
(d) Dielectric relaxation studies

The dielectric dispersion  $\epsilon''$  measured up to 13 . In figs. 6.25-6.29, we have plotted the dielectric loss  $\epsilon''$ , as function of frequency at different temperatures for NPOOB and its mixtures with 9.8%, 26% and 45.5% of OH-EBBA. For the mixture containing 54.5% NPOOB, the measurements in the N and A phases are shown separately (figs.6.28 and 6.29 respectively).

For all the systems studied, the peak value of  $\epsilon''$ , decreases with increase of temperature while the relaxation frequency ( $f_R$ ) given by the maximum value of  $\epsilon''$ , increases. The peak value of  $\epsilon''$ , decreases slowly with temperature in the A phase, and more rapidly in the N phase, essentially reflecting the variation of orientational order parameter in the two phases.

The Cole-Cole plot ( $\epsilon''$ , vs.  $\epsilon'$ ,) in the case of NPOOB is shown in fig.6.30 for a few temperatures. Though the low frequency part of the plot lies on a





**BIG.6.24:** Temperature variations of the low frequency dielectric constants of a mixture of 63.5 mole % of 8 OCB with 36.5 mole % of 40.05 (measured at 1592 Hz). The arrow indicates  $T_{AN}$ .

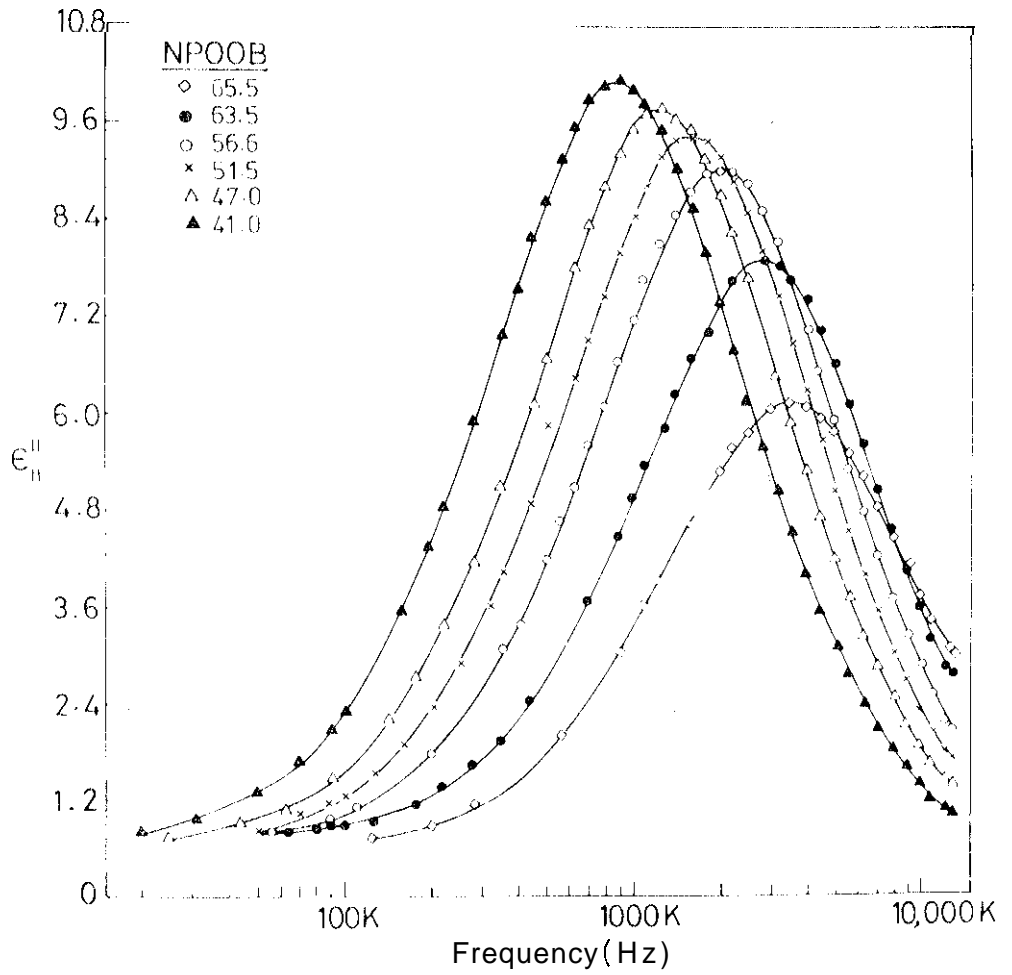


**FIG.6.25:  $\epsilon''$ , as a function of frequency for NPOOB. The numbers against the symbols indicate the temperatures in  $^{\circ}\text{C}$ .**

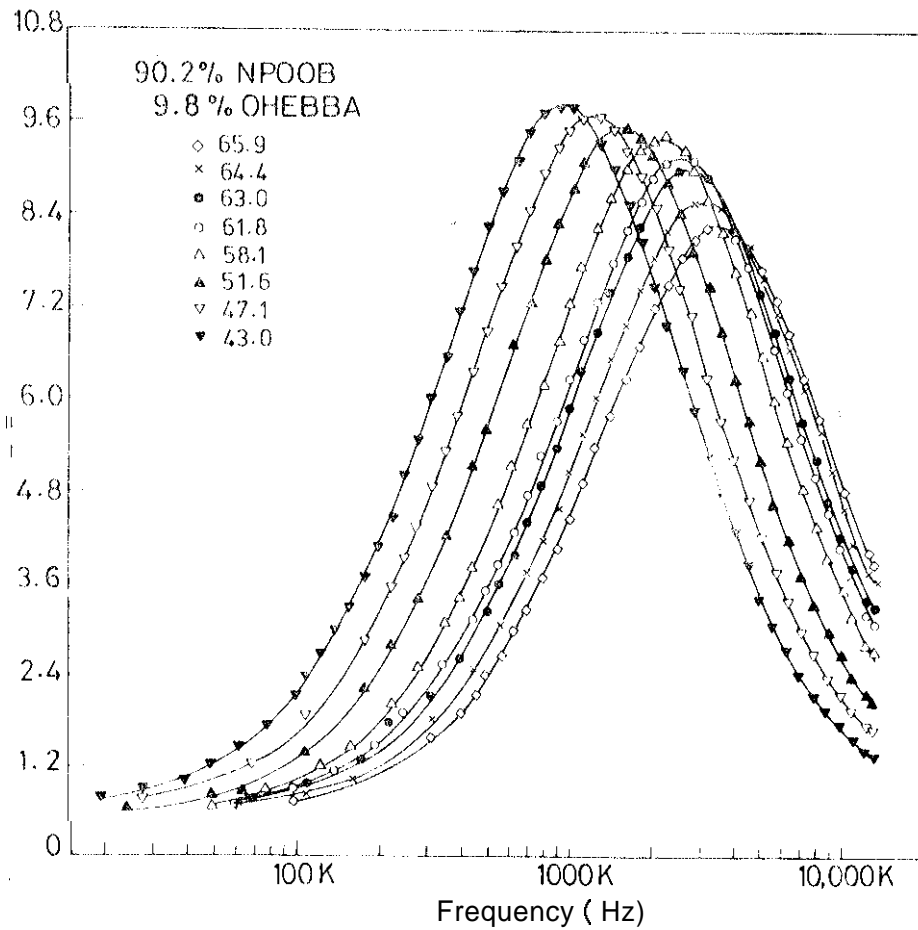


**FIG.6.26:**  $\epsilon''$  as a function of frequency for a mixture of 90.2 mole per cent of NPOOB and 9.8 mole per cent of OH-EBBA. The numbers against the symbols indicate the temperatures in °C.

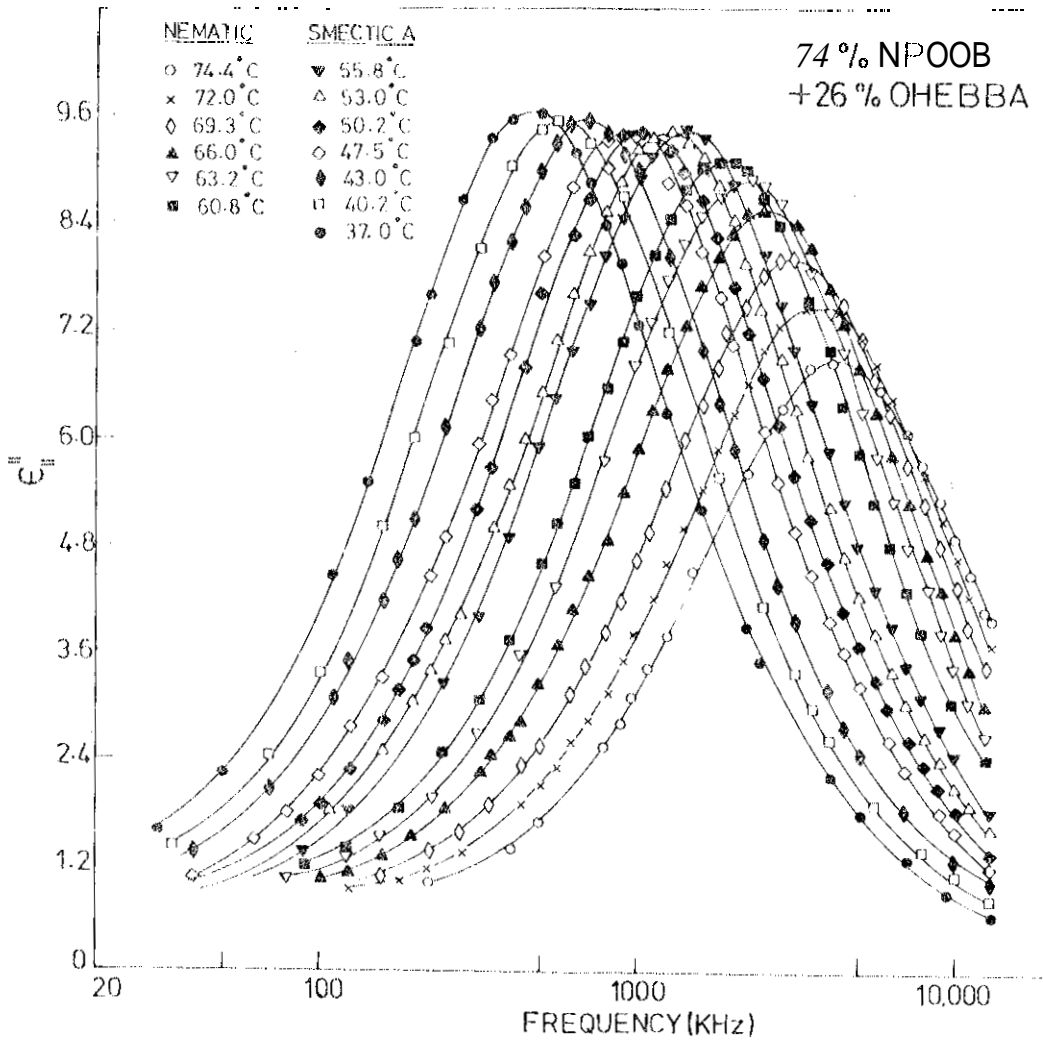
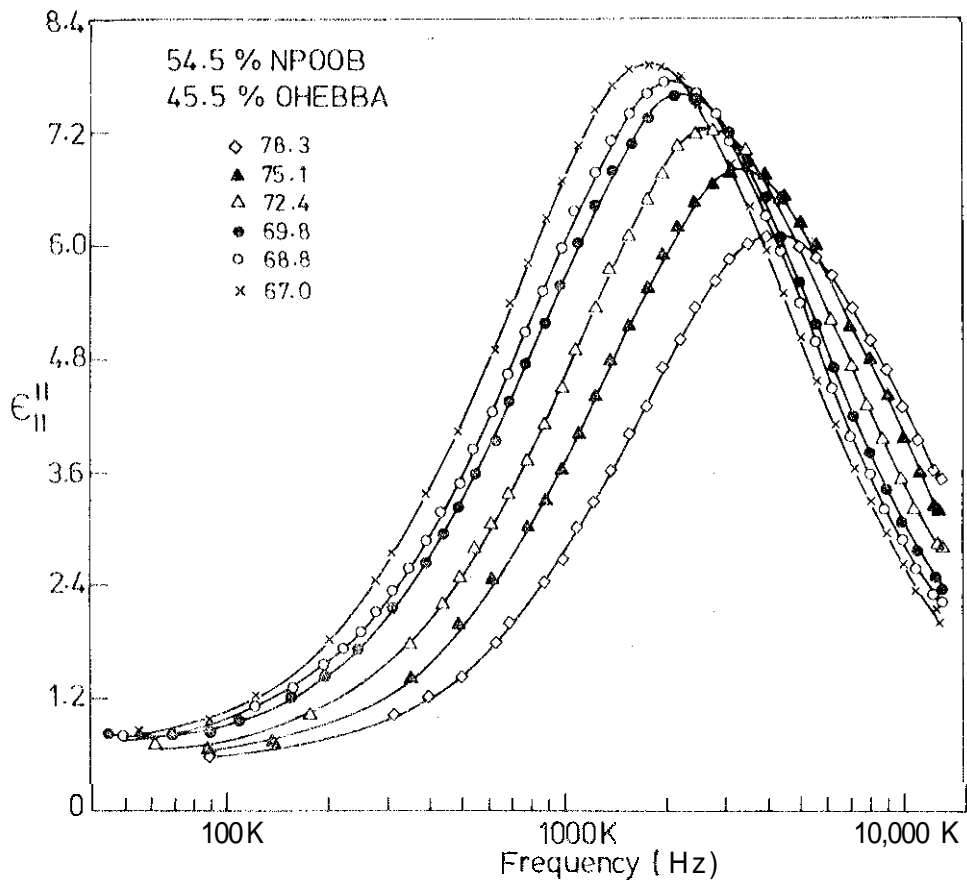


**FIG.6.27:**  $\epsilon''_{11}$  as a function of frequency for a mixture of 74 mole % of NPOOB with 26 mole % of OH-EBBA. The numbers against the symbols indicate the temperatures in °C.



**B16.6.28:** Frequency dependence of  $\epsilon''$  at various temperatures (indicated against the symbols) in the nematic phase of a mixture of 54.5 mole % of NPOOB with 45.5 mole % of OH-EBBA.

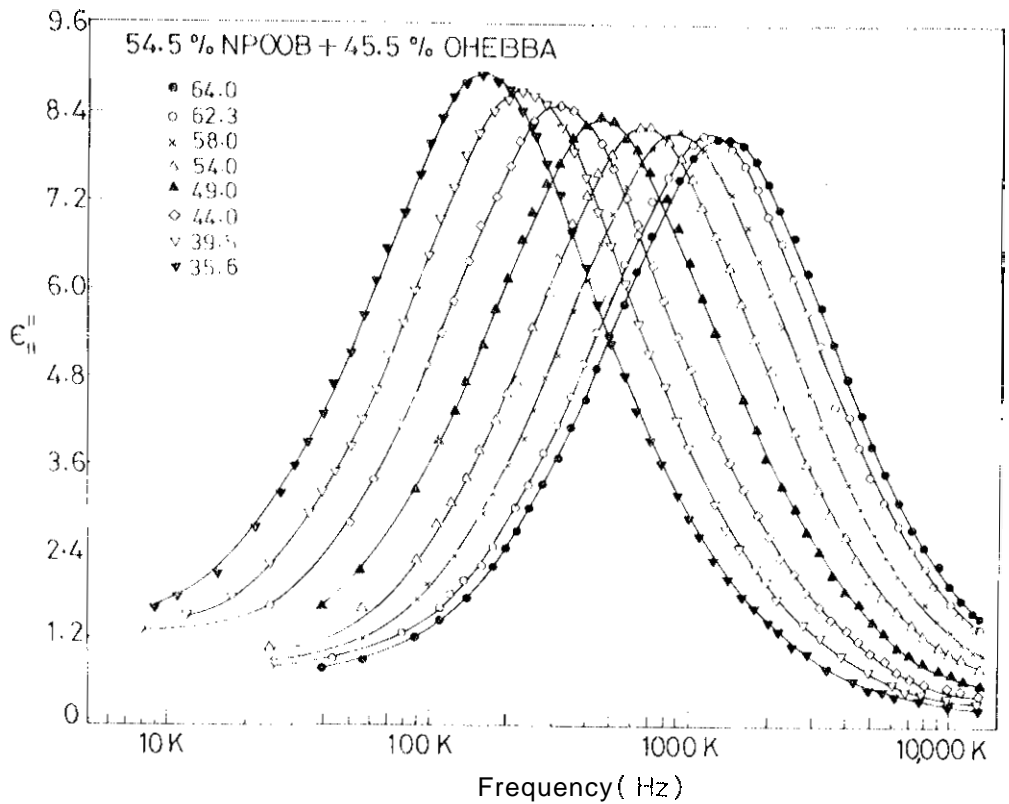


**FIG.6.29: Frequency dependence of  $\epsilon''$  at various temperatures (indicated against different symbols) in the smectic A phase of a mixture of 54.5 mole % of NPOOB with 49.5 mole % of OH-EBBA.**

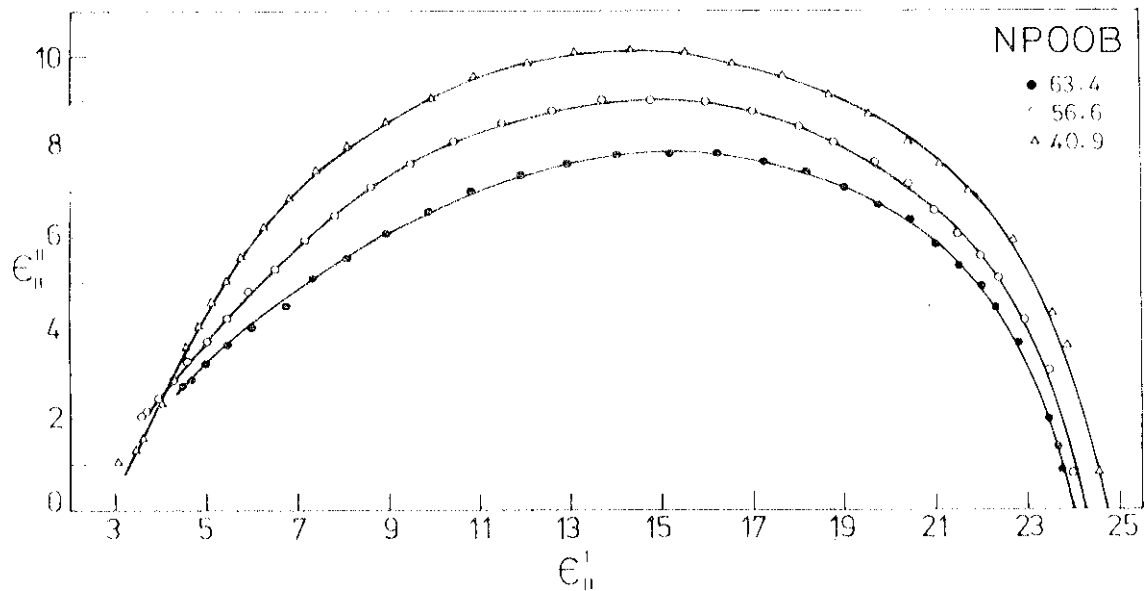


**FIG.6.30:** Cole-Cole plot for  $\epsilon''$ -relaxation in the oaae of NPOOB. The numbers shown against the various symbols indicate the temperatures in °C.

semicircle, there are considerable deviations at higher frequencies. This result is in qualitative agreement with an earlier study on this compound by Bata et al.<sup>38</sup> and indicates a higher frequency relaxation. The latter relaxation may possibly be analogous to the high frequency shoulder found in the  $\epsilon''$  relaxation of 7CB and 7 OCB by Buka et al.<sup>39</sup> This has been attributed by them to @ partial reorientation within short range ordered groups and later reproduced in a numerical calculation on the basis of a model of Brownian motion.<sup>40</sup> Another possible origin for the shoulder lies in the librational and reorientational motion of the transverse dipole moment of the ester group. This relaxation frequency lies at  $\sim 97$  MHz according to reference 38. The latter contribution can be expected to become more important when the orientational order parameter decreases, and indeed as can be seen in fig. 6.30, the high frequency deviations from the semicircular plot are more obvious at higher temperatures.

As described in chapter IV, the relaxation time is given by the equation  $\tau_R = A \exp(w/k_B T)$  where  $\tau_R = 1/2\pi f_R$ ,  $w = q + q_\eta$  is the total activation energy where  $q$  is the nematic potential,  $q_\eta$  is the activation energy due to viscous effects and  $A$  is a constant.



According to this equation, a plot of  $\ln f_R$  vs.  $1/T$  gives a straight line the slope of which is the activation energy. A plot of  $\ln f_R$  vs.  $1/T$  for NPOOB is given in fig.6.31 and the activation energies in the A and N phases (calculated as described above) are given in table 6.4. The values broadly agree with those obtained by Bata et al.<sup>34</sup>

The Cole-Cole plot for the mixture with 90.2% NPOOB is shown in fig.6.32. The peak,  $\omega_{max}$  value is slightly lower than in pure NPOOB (fig. 6.30). The Cole-Cole plot can be better fitted to semicircles at lower temperatures. But considerable deviations are seen at higher temperatures and at higher frequencies. The activation energy (fig.6.33) in the A phase does not change much compared to that of pure NPOOB (table 6.4) but that in the N phase shows some increase.

The Cole-Cole plots for the mixture with 74% NPOOB are shown in fig.6.34 and are broadly similar to those of the previous mixture. The activation energy (fig.6.35) of the A phase is slightly higher than that of 90.2% mixture, while that for the N phase is lowered considerably. Indeed, the activation energy of the N phase has the lowest value (table 6.4) for this mixture which corresponds to the minimum in the phase boundary.

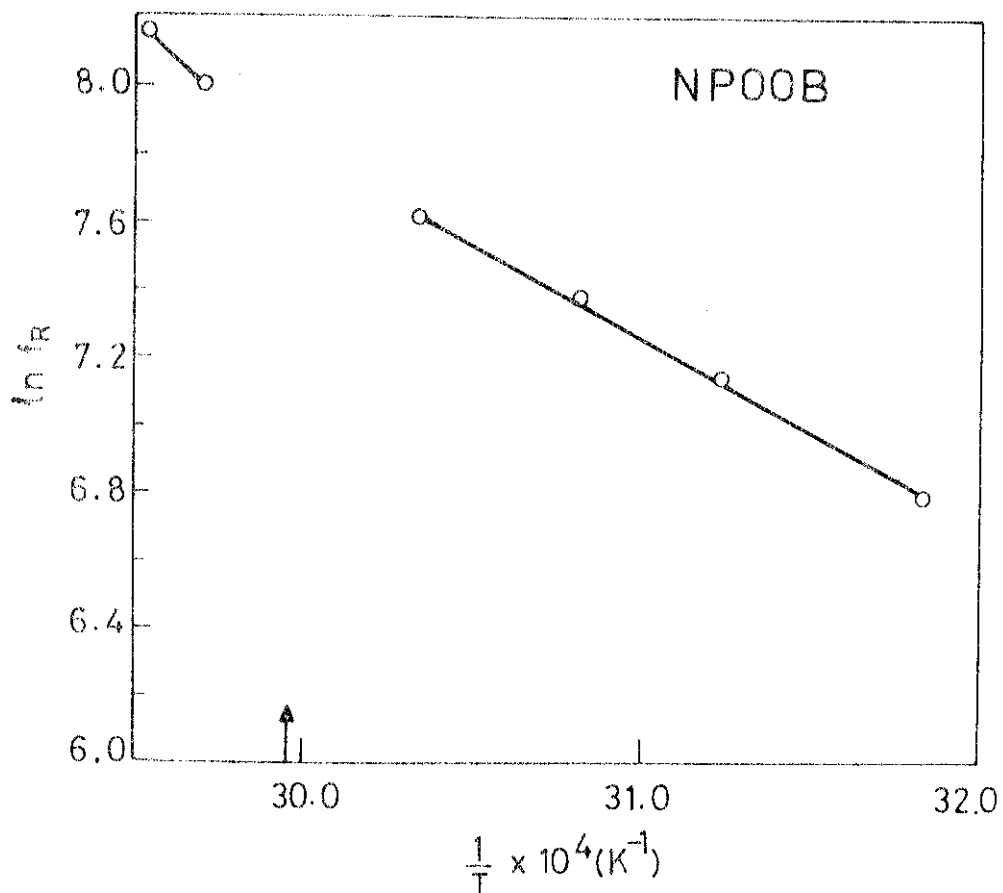


**FIG.6.31:** Plot of  $\ln F_R$  against  $1/T$  in the case of NPOOB where  $f_R$  is the frequency corresponding to  $\epsilon''_i$  peak. The vertical arrow indicates  $T_{AN}$ .

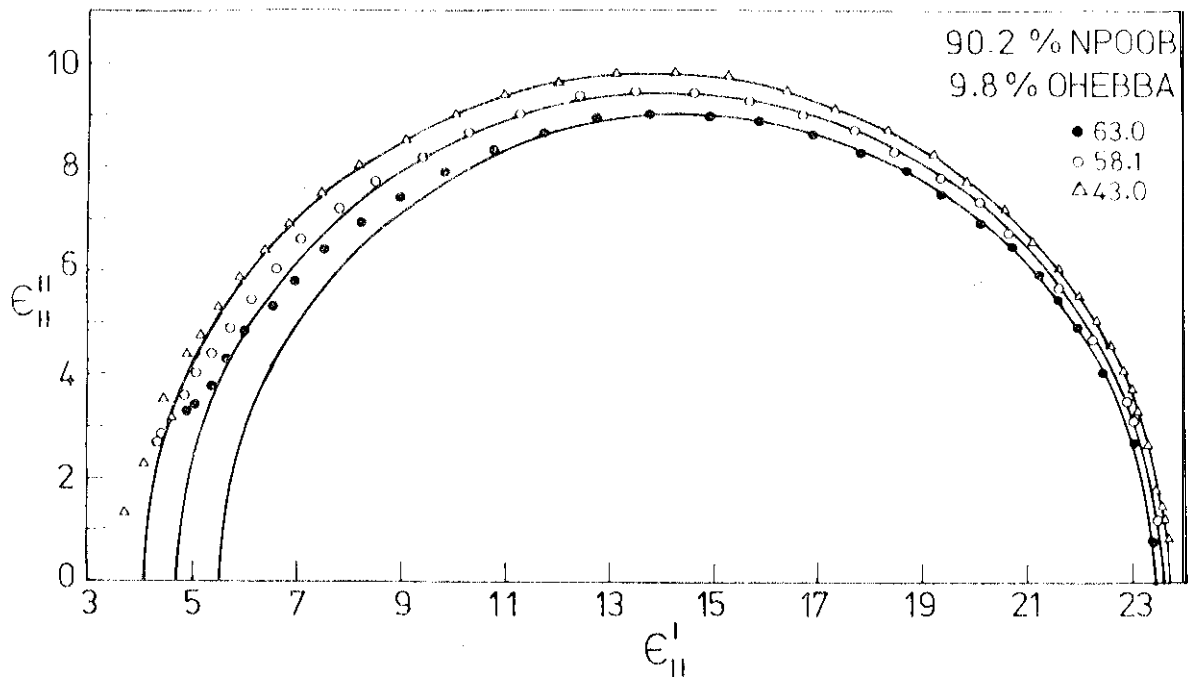


**FIG.6.32: Gale-Cole plot for  $\epsilon_{||}$ -relaxation in the: case of 90.2 mole percent of NPOOB with 9.8 mole % of OH-EBBA at three different temperaturea in °C.**

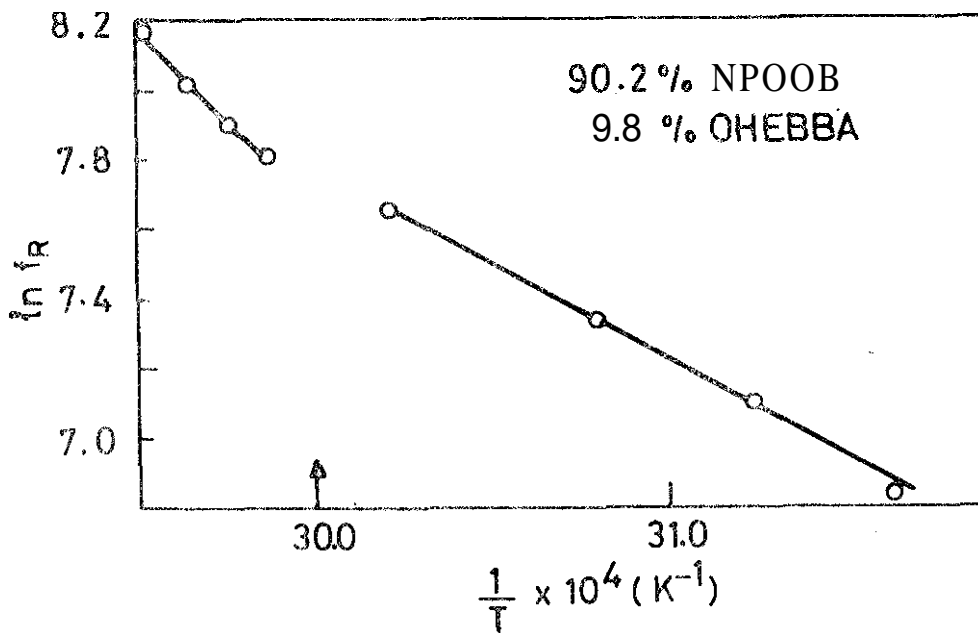


FIG.6.33:  $\ln f_R$  against  $1/T$  for a mixture of 90.2 mole % of NPOOB with 9.8 mole % of OH-BBBA. The vertical arrow indicates  $T_{AN}$ .

- 25 N.V.Madhusudana and S.Chandrasekhar, Proc.Int.Liq. Cryst.Conf., Bangalore, 1973 - Pramana Suppl.1, p.57.
- 26 B.Engelen, G.Heppke, R.Hopf and F.Schneider, Mol.Cryst.Liq.Cryst.Lett. 49, 193 (1979).  
G.Sigaud, F.Hardouin, M.F.Achard and H.Gasparoux, J.de Phys. 40, C3-356 (1979).  
N.V.Madhusudana and K.P.L.Moodithaya, Mol.Cryst. Liq.Cryst. 90, 357 (1983).  
M.Bock, G.Heppke, E.J.Ritcher and F.Schneider, Mol.Cryst.Liq.Cryst. 45, 221 (1978).  
W.L.McMillan, Phys.Rev. A4, 1238 (1971).  
A.Buka, L.Bata and J.Szabon, Presented at the Ninth Int. Liquid Crystal Conf., Bangalore, 1982 - Mol.Cryst.Liq.Cryst. 103, 307 (1983).  
P.E.Gladis, D.Guillon, W.B.Daniels and A.C.Griffin, Mol.Cryst.Liq.Cryst.Lett. 55, 89 (1979).  
M.I.Barnik, S.V.Belyaev, V.G.Rumyatsev, V.A.Tsvetkov and N.M.Shytkov, Forschungen, Uber Flussige Kristalle Ed. D.Demus, Martin-Luther University, Halle (1978)p.84.
- 34 L.Bata and A.Buka, Acta Phys.Polon. A54, 635 (1978).
- 35 G.J.Sprokel, Mol.Cryst.Liq.Cryst. 42, 233 (1977).
- 36 M.Schadt, J.Chem.Phys. 56, 1494 (1972).
- 37 B.R.Ratna, M.S.Vijaya, R.Shashidhar and B.K.Sadashiva, Proc.Int.Liq.Cryst.Conf., Bangalore, 1973 - Pramana Suppl. 1, p.69; Also B.R.Ratna and R.Shashidhar, Pramana 6, 278 (1976).

- 13 J.W.Park, G.S.Bak and M.M.Labes, J.Am.Chem.Soc. 97, 4398 (1975).
- 14 G.S.Oh, Mol.Cryst.Liq.Cryst. 42, 1 (1977).
- 15 A.C.Griffin, R.F.Fisher and S.J.Havens, J.Am.Chem.Soc. 100, 6329 (1978).
- 16 B.Engelen, G.Heppke, R.Hopf and F.Schneider, Ann. Phys. 3, 403 (1978).
- 17 K.P.L.Moodithaya and N.V.Madhusudana, in Liquid Crystals, Proc. Int.Conference, Bangalore, 1979, Ed. S.Chandrasekhar, Heyden, London (1980) p.297; Also see, K.P.L.Moodithaya, 'Optical and Elastic Properties of Liquid Crystals' Thesis, University of Mysore (1981).
- 18 F.Schneider and N.K.Sharma, Z.Naturforsch. 36a, 62 and 1086 (1981) and references given therein.
- 19 J.Szabon and I.Janossy, in Advances in Liquid Crystal Research and Applications, Ed. L. Sata, Pergamon Oxford (1980) p.229.
- 20 J.Szabon and S.Diele, Cryst. Res. Technol. 17, 1315 (1982).
- 21 M.Domon and J.Billard, J.Phys.Paris 40, C3-413 (1979).
- 22 K.A.Suresh, Mol.Cryst.Liq.Cryst. 97, 417 (1983).
- 23 H.K.Sharma, G.Pelzl, D.Demus and W.Weissflog, Z.Phys.Chem. (Leipzig) 261, 579 (1980).
- 24 A.J.Leadbetter, J.C.Frost, J.P.Gaughan, G.W.Gray and A.Mosley, J. de Phys. 40, 375 (1979).

## REFERENCES

- 1 A. Bogojawlensky and N. Winogradoff, Z. Phys. Chemi. 60, 433 (1907).
- 2 A. Bogojawlensky and N. Winogradoff, Z. Phys. Chemi 64, 229 (1908).
- 3 A. Prins, Z. Phys. Chemi 67, 689 (1909).
- 4 R. Walter, Chemi filer., 58B, 2303 (1925).
- 5 J. S. Dave and M. J. S. Dewar, J. Chem. Soc. 4616 (1954); 4305 (1955).
- 6 H. Arnold and H. Sackmann, Z. Phys. Chemi 213, 145 (1960).
- 7 M. J. S. Dewar, J. P. Schroeder and D. G. Schroeder, J. Org. Chem. 32, 1692 (1967).
- 8 E. C. H. Hsu and J. F. Johnson, Mol. Cryst. Liq. Cryst. 20, 177 (1973).
- 9 G. W. Gray, K. J. Harrison and J. A. Nash, Proc. Int. Liquid Cryst. Conf., Bangalore, 1973, Pramana Suppl. 1, p. 381.
- 10 H. Sackmann and D. Demus, Z. Phys. Chemi. (Leipzig) 224, 177 (1963).
- 11 J. S. Dave, K. L. Patel and K. L. Vasanth, Indian J. Chem. 4, 505 (1966).
- 12 G. Pelsl, D. Demus and H. Sackmann, Z. Phys. Chem. (Leipzig) 238, 22 (1968).

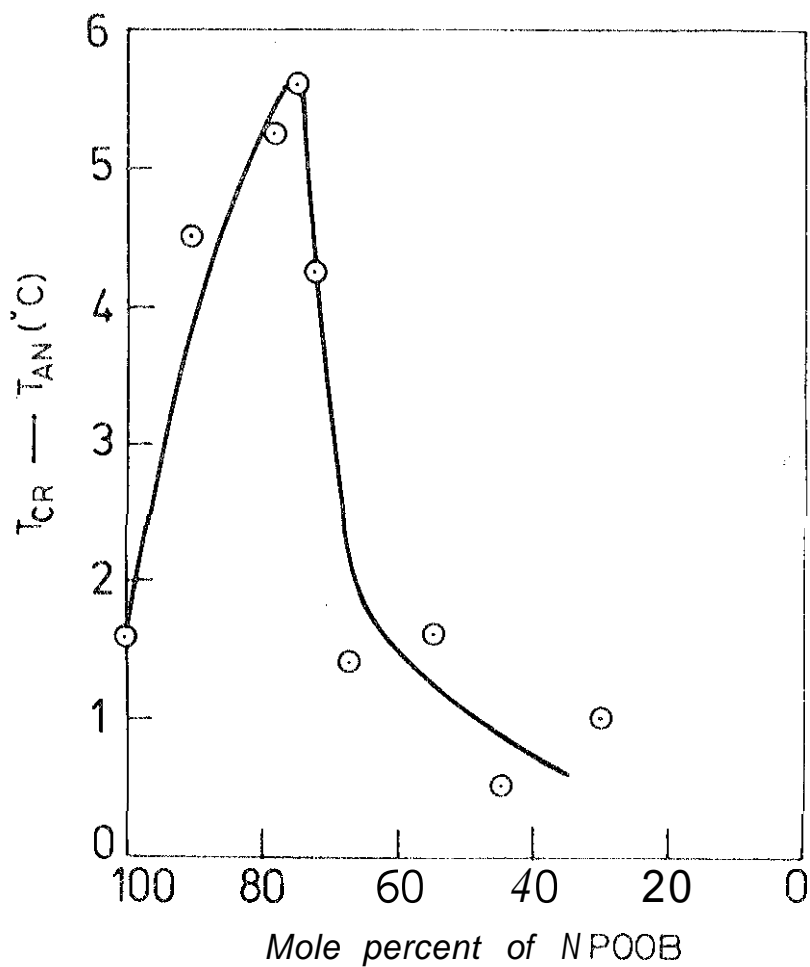


**FIG.6.48:** Composition-dependence of the relative cross over temperatures of the conductivities of mixtures of HPOOB with CH-EBBA



compositions close to the maximum in the A-N transition boundary, especially at lower temperatures (see table 6.5). The fact that the A-N transition is very weak for the composition corresponding to the minimum in the A-N boundary and becomes stronger on either side of this composition is reflected in the cross over temperature ( $T_{Gr}$ ) of the conductivity anisotropy. As seen in fig. 6.48,  $T_{Gr} - T_{AN}$  shows a strong peak for the composition corresponding to the minimum in the, A-N boundary, since the smectic like short range order fluctuations are very strong in this case even at temperatures a few degrees above  $T_{AN}$ .

In conclusion, the competition between two types of interactions, viz., charge transfer complex formation between the highly polar and weakly polar molecules and the antiparallel interaction between the highly polar molecules gives rise to some interesting variations of physical properties of the mixture that we have studied.

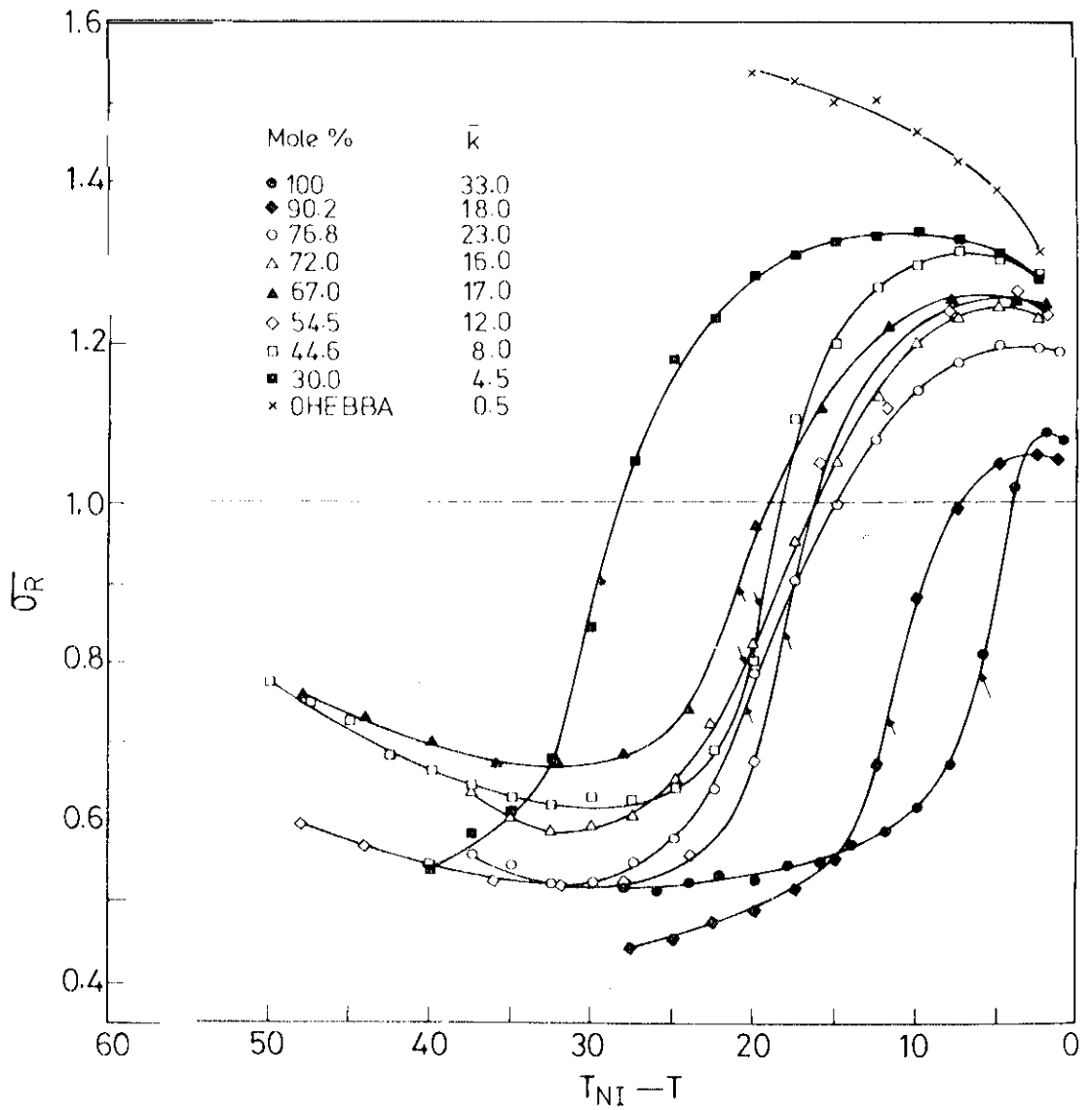
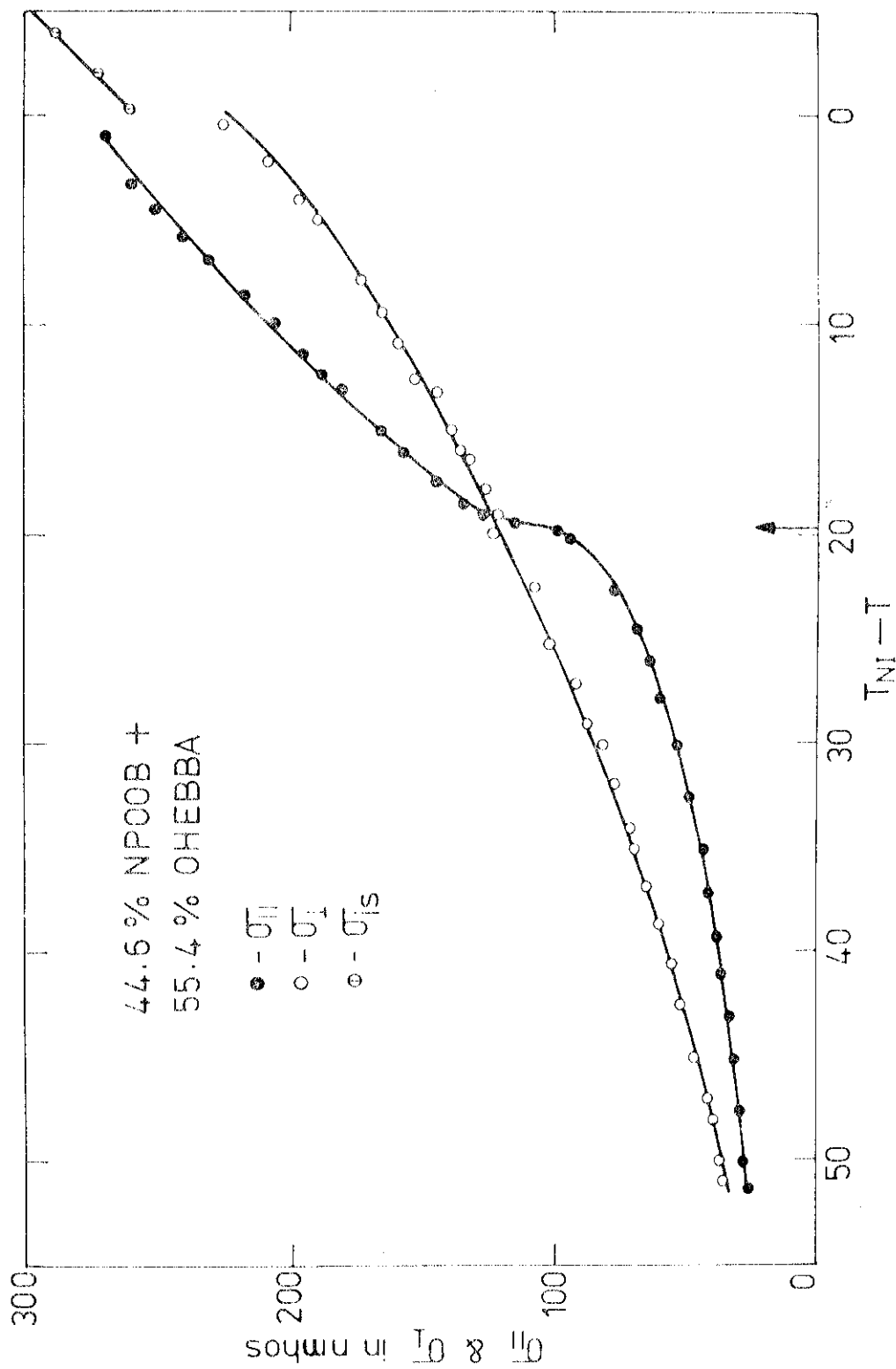


FIG.6.47: The ratios of the principal conductivities  $\sigma_R = \sigma_{11}/\sigma_{12}$  of various mixtures of NPOOB with OH-EBBA as functions of relative temperature. The first number against each symbol is the mole percentage of NPOOB and the second number the mean specific conductivity  $\bar{k} \times 10^9$  (oh. cm) $^{-1}$  at 76°C. The arrows indicate  $T_{AN}$ .

in fig.6.47. The diagram is somewhat complicated, mainly because of the peculiar shape of the A-N boundary. Further, as mentioned in chapter V,  $\sigma_R$  depends on the nature and concentration of the conducting impurities, the value of  $\sigma_R$  generally going up if the medium has higher conductivity.<sup>44,45</sup> The conducting impurities in our samples are unknown, and in fig.6.47 we have given the values of the mean specific conductivity  $\bar{K}$  at a common temperature (76°C) for all the systems studied.  $\bar{K} = (\lambda'/A)\bar{\sigma}$  where  $\lambda'/A$  the geometrical parameter of the cell was determined from the measured value of the capacitance of the empty cell and  $\bar{\sigma}$  is the measured conductivity if the medium is in the isotropic phase, or  $\bar{\sigma} = (\sigma_{||} + 2\sigma_{\perp})/3$ , if it is in the N phase. It is clear that NPOOB has a much higher value of  $\bar{K}$  than OH-EBBA, the mixtures having some intermediate values.

We can notice a few features: (i) Understandably,  $\sigma_R$  falls more steeply in the cases where the A-N transition is of first order character compared to the ones where it has a second order nature. (ii) For a wide range of compositions (between 76.8% to 44.6% NPOOB),  $\sigma_R$  value shows a broad minimum at  $T_{NI} - T \approx 32^\circ\text{C}$  and starts increasing as the temperature is lowered further. This is probably connected with decrease of  $f_R$  to very low values for



**FIG. 6.46: Temperature variations of the principal conductivities of a mixture of 44.6 mole per cent of NPOOB with 55.4 mole per cent of OH-EBBA. The vertical arrow indicates  $T_{NI}$ .**

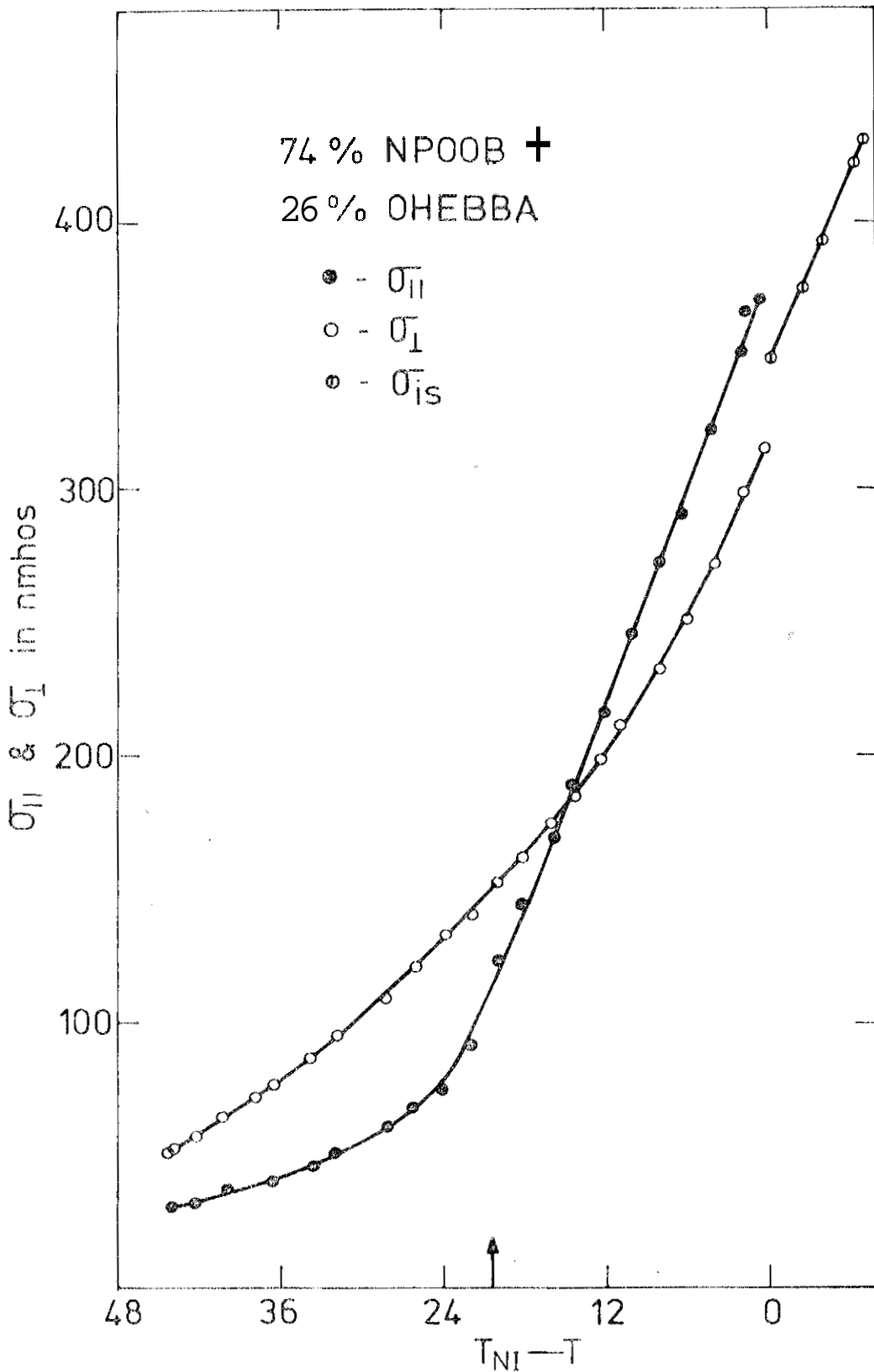


**FIG.6.45:** Temperature variations of the principal conductivities of a mixture of 74 mole per cent of NPOOB with 26 mole per cent of OH-EBBA. The vertical arrow indicates  $T_{AN}$ .

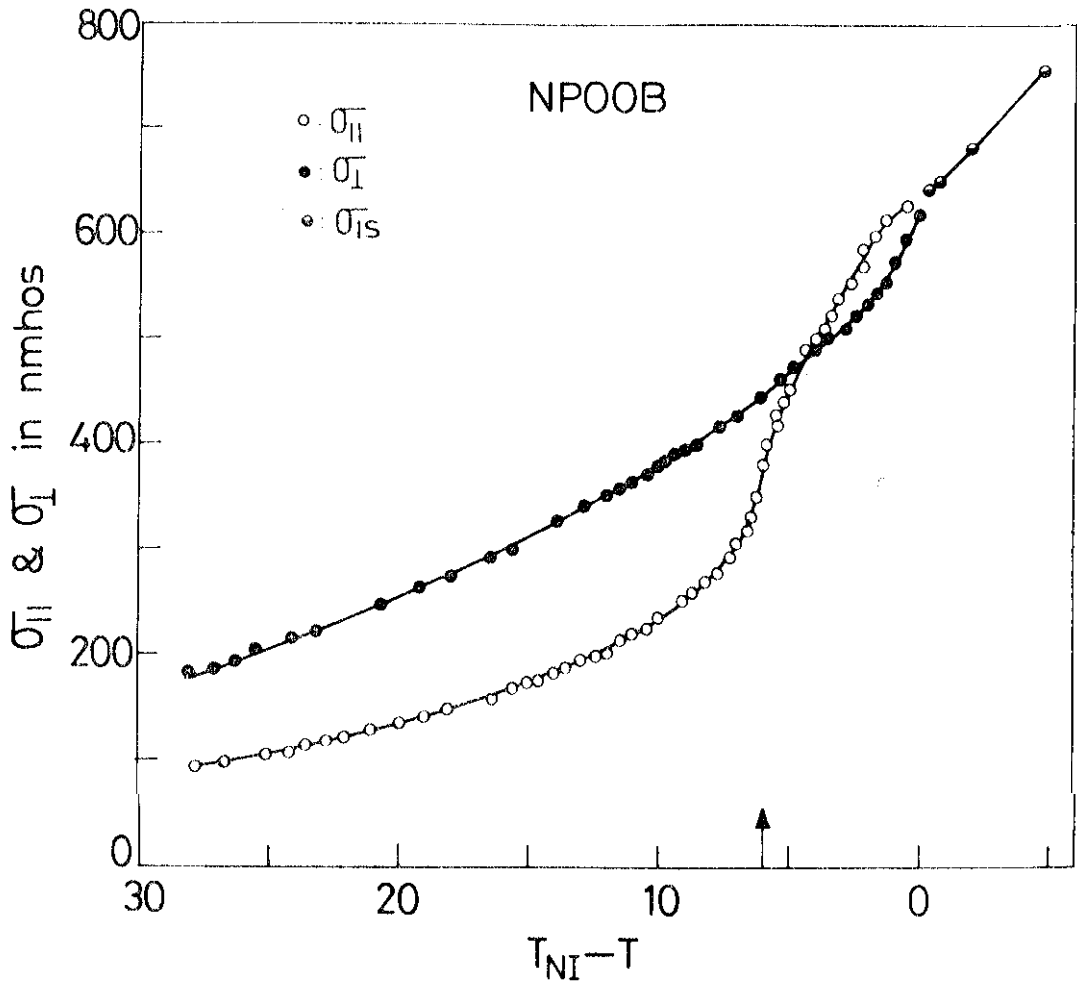


**FIG. 6.44:** Temperature variations of We principal conductivities of NPOOB. The vertical arrow indicates  $T_{AN}$  ■

becoming negative a few degrees above  $T_{AN}$  as is to be expected<sup>43,44</sup> (for an introduction and discussion of earlier results on conductivity studies of liquid crystals, see chapter V). As discussed in the previous chapter, in the A phase ions can flow more easily in the plane of the layers than perpendicular to the planes. Therefore, the conductivity perpendicular to the director ( $\sigma_{\perp}$ ) is greater than the conductivity parallel to the director ( $\sigma_{\parallel}$ ) in the A phase.  $\sigma_{\parallel}$  exhibits 'jump' at  $T_{AN}$  for both NPOOB (fig.6.44) and the mixture with 44.6% NPOOB (fig.6.46). This is caused by the fact that the A-N transition has a first order character in both the cases (fig.6.6). On the other hand,  $\sigma_{\perp}$  falls steeply up to  $T_{AN}$  in the case of the mixture with 74% NPOOB and then levels off in the A phase (fig.6.45), since the A-N transition in this case is almost of second order character. On the other hand,  $\alpha$  varies smoothly across  $T_{AN}$  for all the compositions studied. This difference in the variations of  $\sigma_{\parallel}$  and  $\alpha$  has already been discussed in chapter V in terms of the permeation process due to the layering in the A phase which contributes to a lowering of  $\sigma_{\parallel}$ .

The temperature variations of the conductivity ratio  $\sigma_R = \sigma_{\parallel} / \sigma_{\perp}$  are shown for all the systems studied,

$\epsilon_{\parallel}$  in the N phase compared to that in the A phase leads to a lower activation energy in the latter phase; and (b) possible influence of anisotropic packing effects in the A phase.

Indeed in system I, the smallest difference between the activation energies of the A and N phases occurs for the mixture with 74 mole per cent of NPOOB mainly because of the low value in the N phase. Further, as we have seen earlier (fig. 6.12), this mixture has the maximum thermal expansion coefficient of layer spacing. As we discussed in chapter IV, in such a case the anisotropic packing is less effective in lowering the activation energy in the A phase. This could also contribute to a reduction in the difference in activation energies between the A and N phases of this mixture.

#### (c) Conductivity Studies

The principal conductivities ( $\sigma_{\parallel}$  and  $\sigma_{\perp}$ ) of three representative compositions are shown in figs. 6.44 - 6.46. (We have measured conductivities in all the systems mentioned earlier, but only three representative diagrams are presented here.)

In all the cases, as the sample is cooled, the conductivity anisotropy ( $\Delta\sigma = \sigma_{\parallel} - \sigma_{\perp}$ ) changes sign



in the case of system I (NPOOB-OHEBBA). Thus the induced A phase is stable over a much wider range of temperatures in system II than in system I. The interactions are strong at lower temperatures, and the activation energy has a high value. As the temperature is raised, the interactions are weakened giving a lower activation energy. Further, the reorientation process takes non-Debye characteristics (fig.6.41) indicating a complex mechanism. The environment of 3 CCB molecules is probably no longer as well defined as at lower temperatures.

The activation energy in the N phase is lowest for the mixture corresponding to the minimum in the A-N boundary. This is probably a consequence of the nearly second order A-N transition in this case (fig.6.6). The N phase will have strong smectic like short range order in this case which is reflected in the low activation energy of the N phase. As we have discussed in chapter IV, layering leads to a lowering of the activation energy.

As in other systems discussed in chapter IV, the activation energies in these systems also are lower in the A phase than in the N phase. The origin of this phenomenon has been discussed in chapter IV in terms of (a) a recent theory of Edwards and Madden<sup>42</sup> according to which the larger temperature variation of low frequency

fair to assume that the strongly polar NPOOB molecules contribute almost entirely to the observed dielectric relaxation of the mixtures. Thus the observed increase in the activation energy of the mixture compared to that of pure NPOOB should be attributed to the formation of NPOOB-OHEBBA pairs. This interaction is also responsible for the large reduction of the relaxation frequency itself in the mixtures (see table 6.5). In order to participate in the relaxation process, an NPOOB molecule has to either carry the OH-EBBA molecule with which it has formed a molecular complex or break away from the pair. Further, the Cole-Cole plots show that at lower temperatures the mixtures deviate very little from a Debye relaxation (fig.6.36). Thus the short range order effects in NPOOB-OHEBBA pairs do not lead to any tail in the high frequency region. As the temperature is increased, more NPOOB-NPOOB pairs are formed and further, the orientational order parameter decreases thus  $\mu_t$ -reorientational motion better visible in the  $\epsilon''$  measurement and the high frequency tail is again noticeable.

As argued earlier, the interactions between NPOOB - 40.05 molecules of system II leading to the formation of the induced A phase are much stronger than

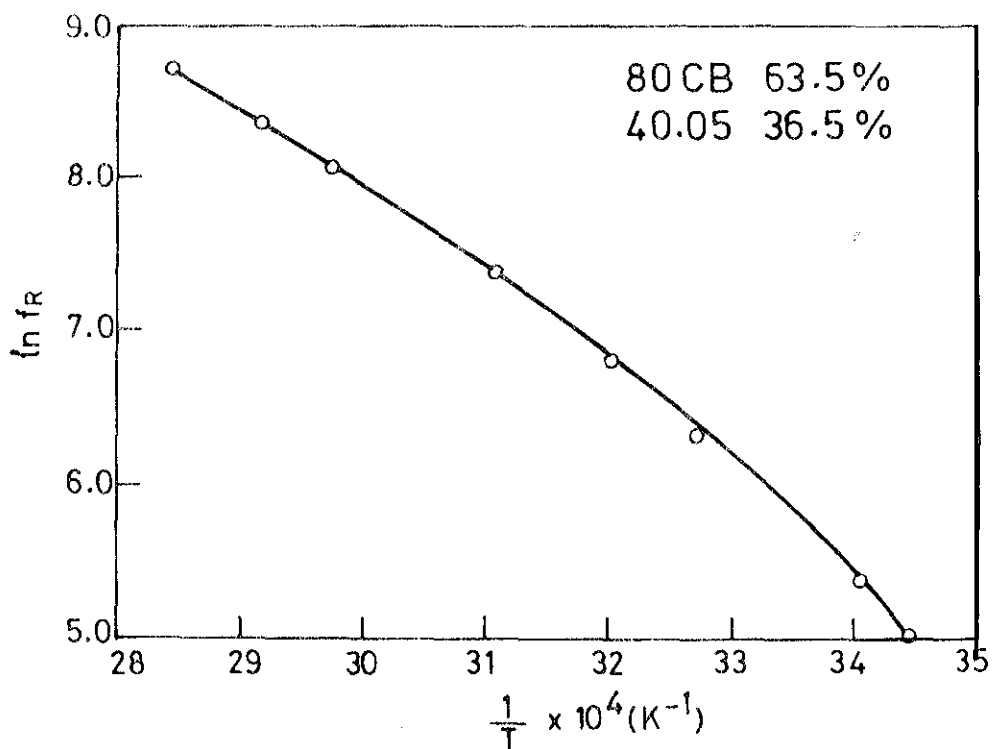


**FIG.6.43:** Plot of  $\ln f_R$  vs.  $1/T$  in the case of a mixture of 63.5 mole per cent of 8 OCB with 36.5 mole per cent of 40.05, where  $f_R$  is the frequency corresponding to  $\epsilon''$  peak.

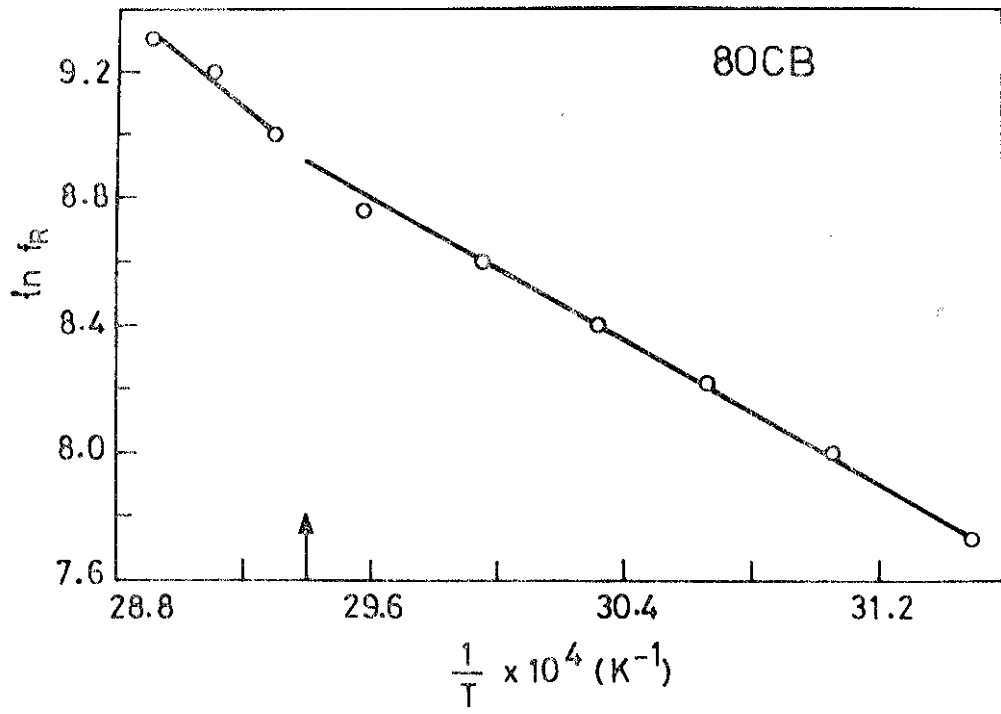


FIG.6.42: Plot of  $\ln f_R$  ve.  $1/T$  in the case of 8 0CB, where  $f_R$  is the frequency corresponding to  $\epsilon''$  peak. The vertical arrow indicates  $T_{AN}$  .

ester dipole moment adds to the total dipole moment of *the* molecule and gives rise to a higher peak value. The activation energies calculated from  $\ln f_R$  vs.  $1/T$  plots (figs. 6.42 and 6.43) are listed in table 6.4 along with the data of system 1. The activation energy in the  $\alpha$  phase is smaller than that in the  $N$  phase in S OCB also. In the case of the mixture of S OCB with 40.05 (fig. 6.41) the Cole-Cole plot is a good semicircle with the centre lying on the  $\epsilon'$  axis only at lower temperatures. At higher temperature, the centre of the circular arc lies below the  $\epsilon'$  axis which indicates a relaxation involving a distribution of relaxation times.<sup>41</sup> Indeed, the plot of  $\ln f_R$  vs  $1/T$  (fig. 6.43) does not field a straight line as in other cases, but a line curved such that the activation energy which is  $\sim 0.43$  eV at the highest temperature in the  $A$  phase continuously increases to  $\sim 0.87$  eV at the lowest temperature of measurement.

As discussed in earlier sections, in system I the NPOOB and OH-EBBA molecules tend to form interacting pairs (due to charge-transfer complex formation and other interactions) in the mixtures. The pairs are likely to break up at higher temperatures, thus allowing NPOOB molecules to form antiparallel pairs. It is perhaps

**Table 6.5(continued)**

	Temperature °C	f <sub>R</sub> (KHz)
54.5% NPOOB + 45.5% OH-EBMA	78.3	4400
	75.1	3200
	72.4	2800
	69.8	2250
	68.8	2150
	67.0	1800
	64.0	1350
	62.3	1150
	58.1	880
	54.0	660
	49.0	450
	44.0	310
	39.5	220
35.6	160	
8 OCB	73.1	11000
	70.7	9800
	68.4	8000
	65.1	6400
	60.9	5500
	56.8	4500
	53.3	3750
	49.0	3000
	44.5	2300
63.5% 8 OCB + 36.5% 40.05	78.8	6000
	70.0	4300
	63.4	3200
	48.8	1600
	39.3	900
	32.7	560
	20.7	220
17.5	155	

**Table 6.5****Relaxation Frequencies**

	Temperature °C	$f_R$ (KHz)
NPOOB	65.5	3500
	63.5	2850
	56.6	2050
	51.5	1600
	47.0	1250
	41.0	880
90.2% NPOOB + 9.8% OH-EBBA	65.9	3500
	64.4	3050
	63.0	2700
	61.8	2500
	58.1	2100
	51.6	1550
	47.1	1200
	43.0	920
74% NPOOB + 26% OH-EBBA	74.4	4400
	72.0	3600
	69.3	3100
	66.0	2500
	63.2	2200
	60.8	1850
	55.8	1400
	53.0	1250
	50.2	1050
	47.5	900
	43.0	700
	40.2	580
37.0	470	

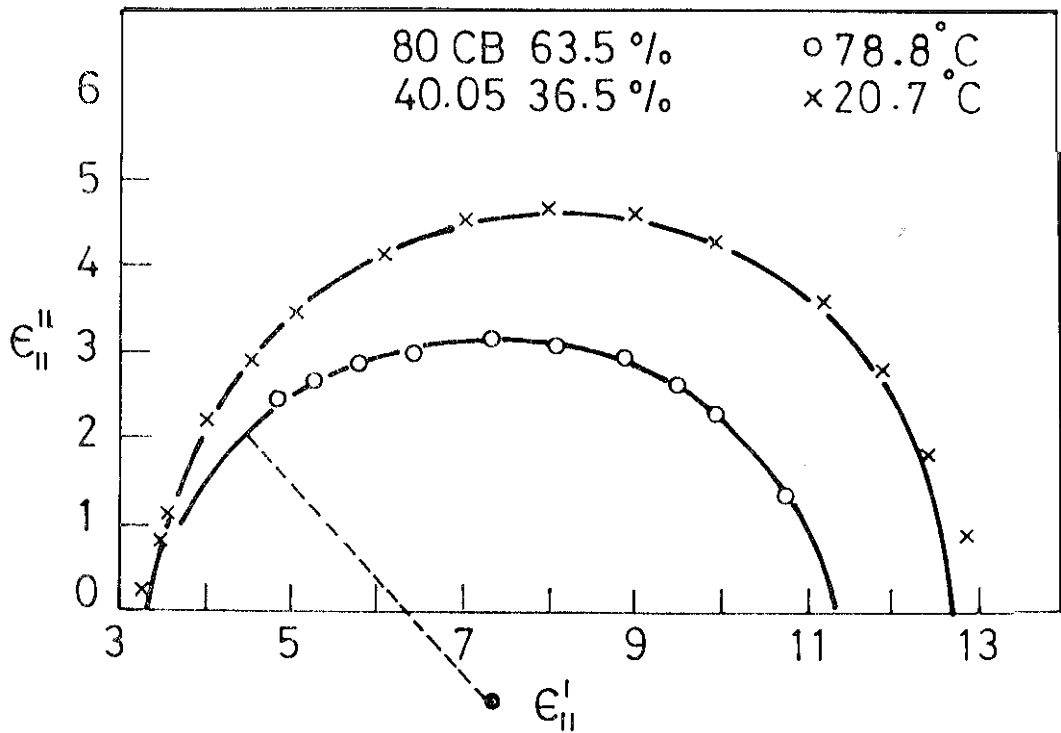


**FIG.6.41:** Cole-Cole plot for  $\epsilon''_{11}$ -relaxation in the case of a mixture of 63.5 mole % of 8 OCB and 36.5 mole % of 40.05. Centre of the semicircle corresponding, to 20.7°C lies on the  $\epsilon'_{11}$  axis while that corresponding to 78.8°C lies below the  $\epsilon'_{11}$  axis.



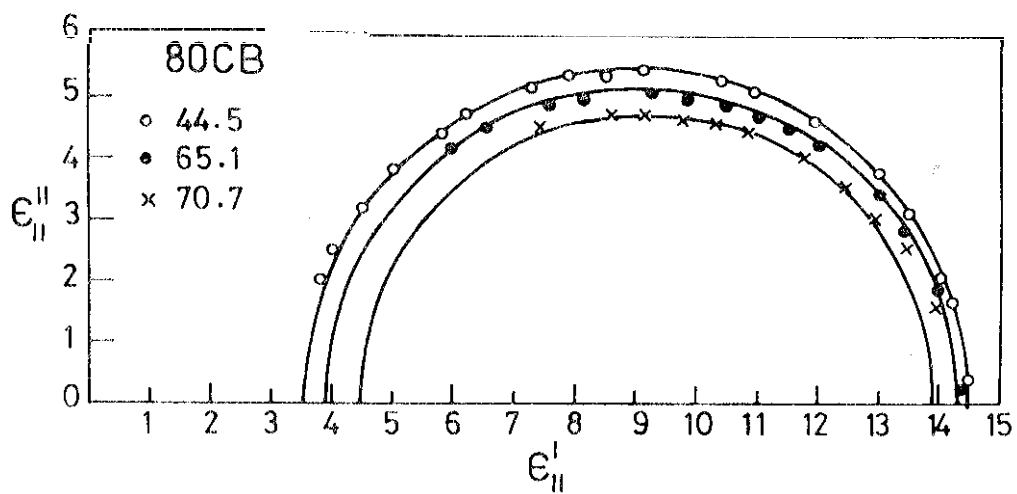


**FIG.6.40: Cole-Cole plots for  $\epsilon_1$ -relaxation in the case of 8 OCB at 44.5°C (○), 65.1°C (●) and 70.7°C (x).**

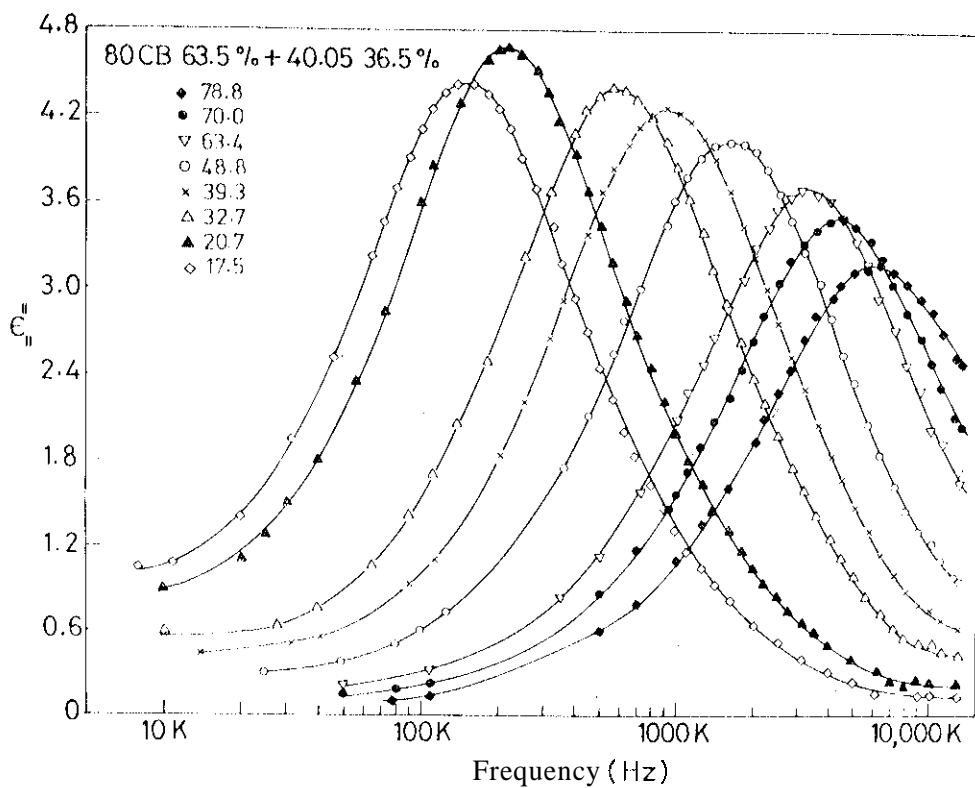


**FIG.6.39:**  $\epsilon''$ , as a function of frequency for a mixture of 63.5 mole % of 8 OCB and 36.5 mole % of 40.05. The numbers against the symbols indicate temperatures in °C.

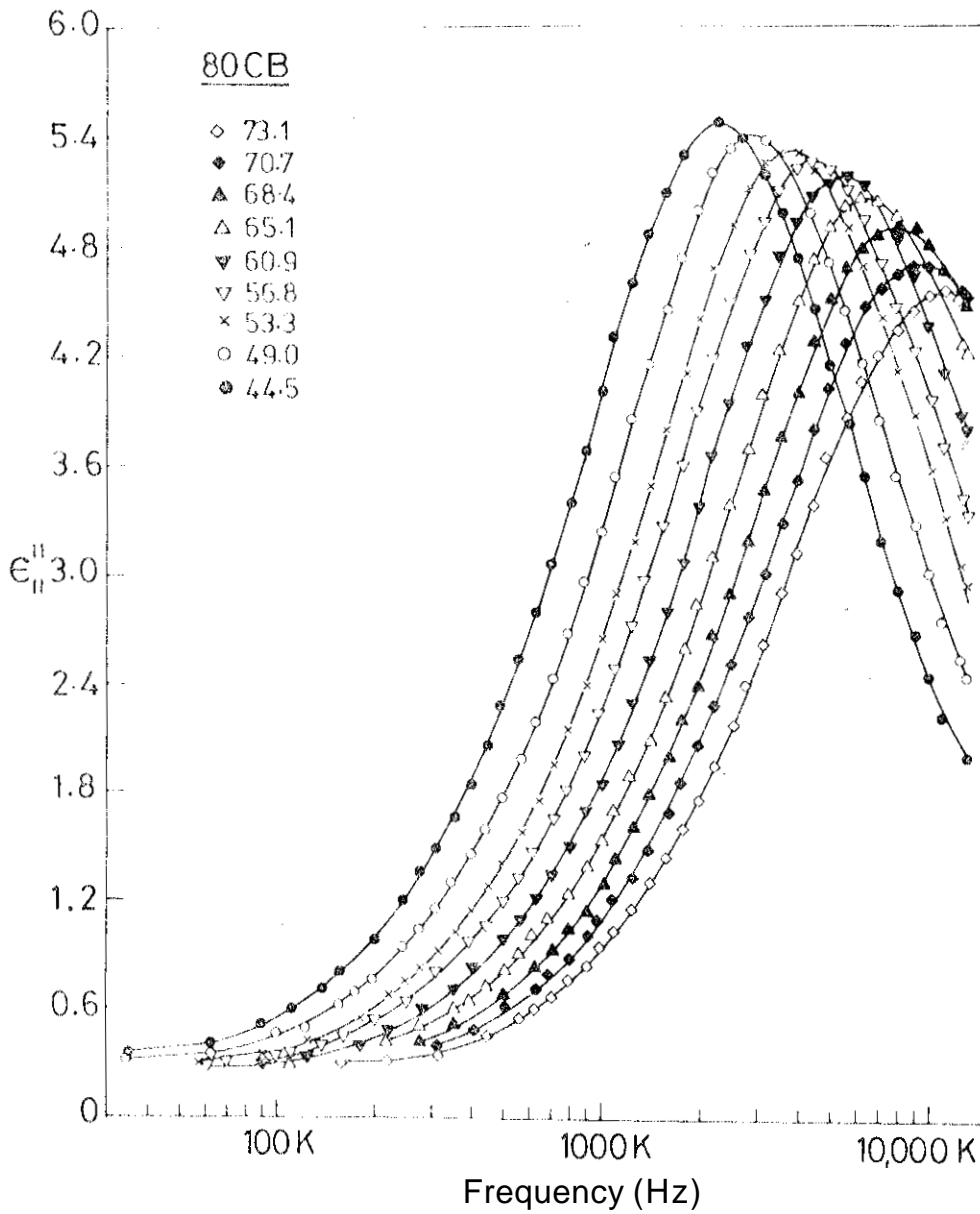


**FIG.6.38:** Frequency dependence of  $\epsilon''_{||}$  at various temperatures (indicated against the symbols) in the case of 80CB.

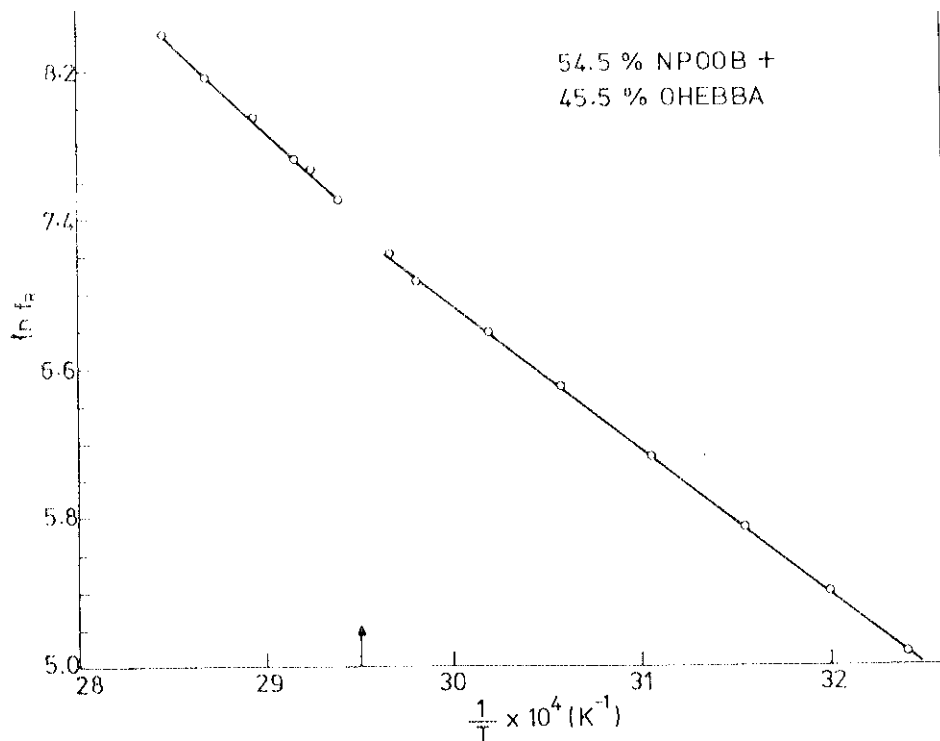


**FIG.6.37:** Plot of  $\ln f_R$  vs.  $1/T$  in the case of a mixture of 54.5 mole % of HPOOB and 45.5 mole % of OH-EBBA, where  $f_R$  is the relaxation frequency. The arrow indicates  $T_{AN}$ .

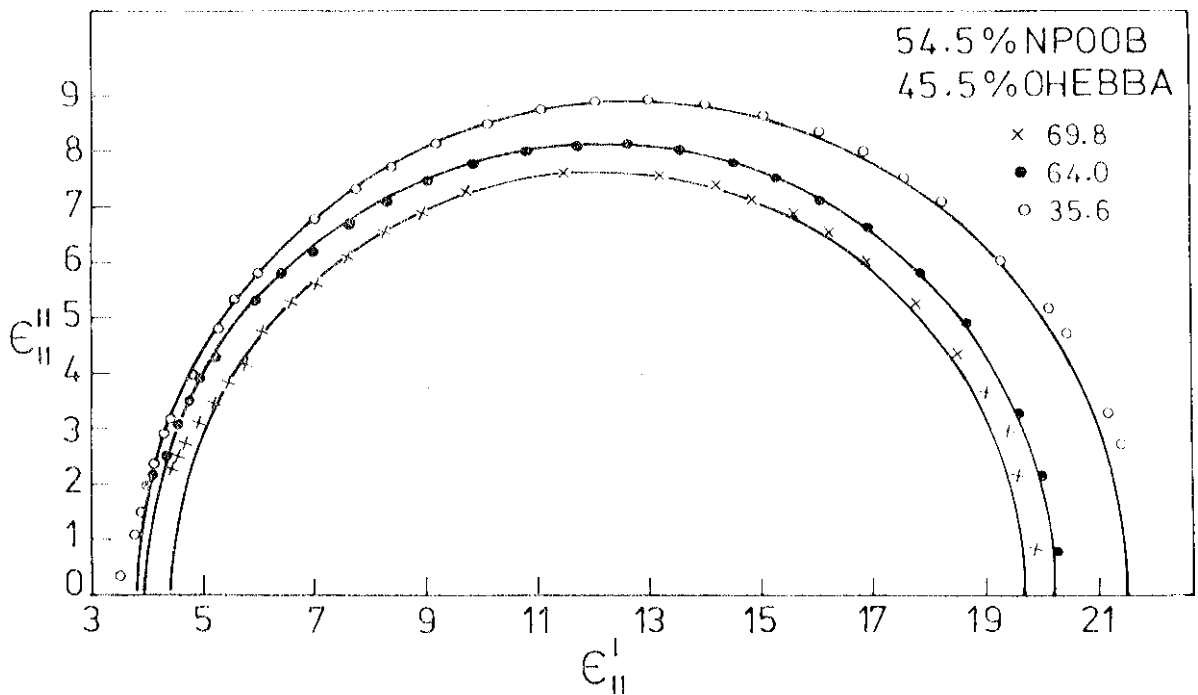


**FIG.6.36: Cole-Cole plots for  $\epsilon_{||}$ -relaxation in the case of 54.5 mole % of NPOOB with 45.5 mole % of OH-EBBA drawn at different temperatures ( $^{\circ}\text{C}$ ) indicated against the symbols.**

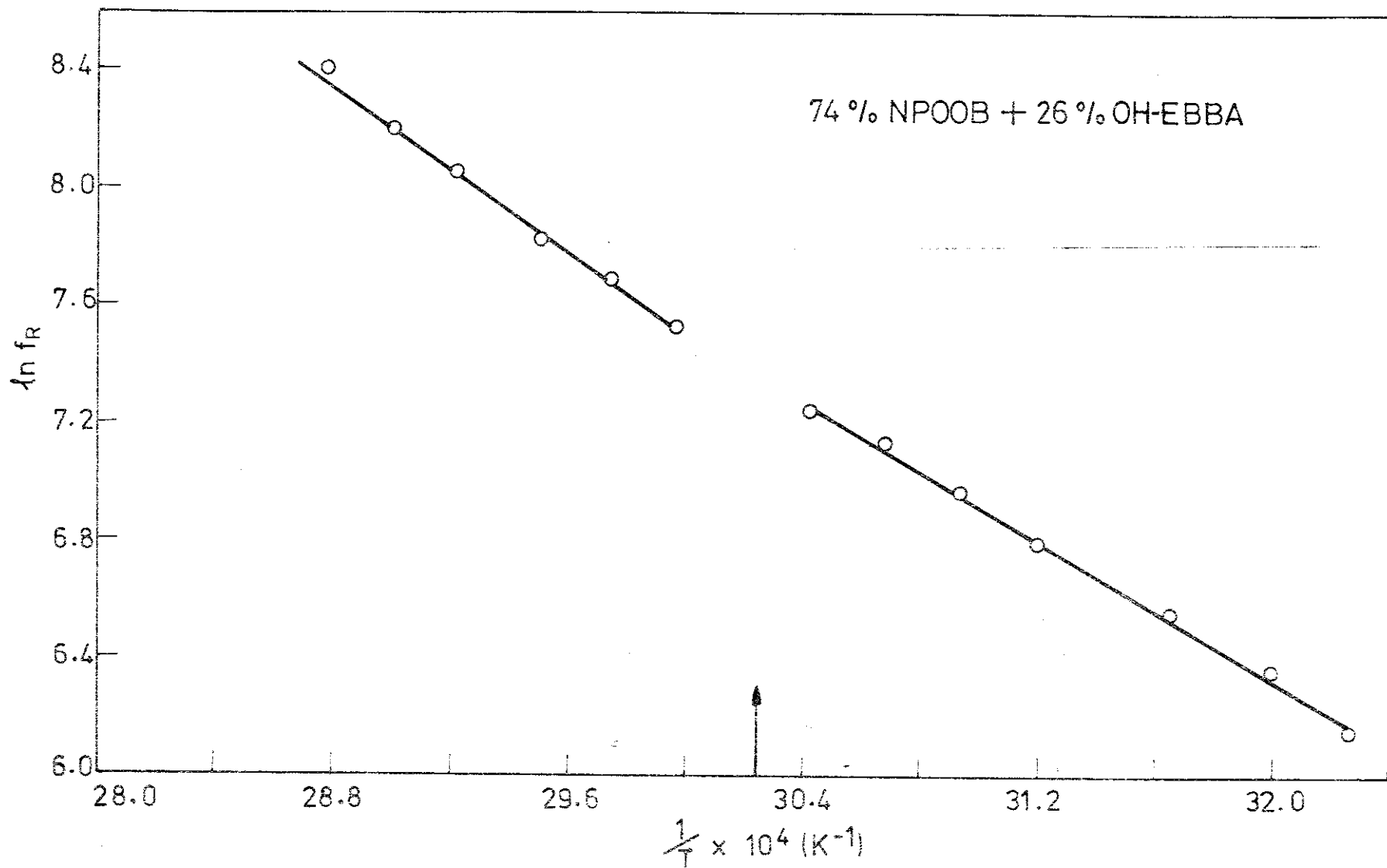
The Cole-Cole plot for a mixture with 54.5% NPOOB which is close to the composition corresponding to the maximum in We 6-31 boundary is shown in fig.6.36. The fit with a semicircle is now very good indicating that a single relaxation characterizes the dispersion. The frequency of the  $\epsilon''$  peak at  $\sim 40^\circ$  is  $\sim 200$  KHz for the 54.5% mixture while it is  $\sim 900$  KHz for pure NPOOB. The activation energy in the A phase has increased considerably for this mixture (fig.6.37, table 6.4) compared to that of pure NPOOB.

The plots of dielectric loss ( $\epsilon''$ ) versus frequency for 8 OOB and its mixture with 36.5% of 40.05 one shown in figs.6.38 and 6.39. The  $\epsilon''$  peak value generally decreases with increase of temperature, except in the mixture, the  $\epsilon''$  peak is lowered at the supercooled temperature of  $17.5^\circ\text{C}$ . We cannot rule out the possibility of a partial crystallization during the experiment in this case. The relaxation frequencies ( $f_R$ ) [corresponding to the peak values of  $\epsilon''$ ] at various temperatures are listed in table 6.5. Cole-Cole plots for these systems are shown in figs.6.40 and 6.41. In 8 OOB, the Cole-Cole plots are semicircles. The peak value of  $\epsilon''$  is  $\sim 5.4$  at the lowest temperature which is much lower than that in NPOOB (fig.6.30). In the latter compound the

Table 6.4

Activation energies in eV in smectic A and  
nematic phases

	<u>Smectic A</u>	<u>Nematic</u>
NPOOB	0.47	0.77
90.2% NPOOB + 9.8% OH-EBBA	0.47	0.86
74% NPOOB + 26% OH-EBBA	0.51	0.62
54.5% NPOOB + 45.5% OH-EBBA	0.67	0.83
8 OCB	0.49	0.7
63.5% 8 OCB + 36.5% 40.05	increases continu- ously from 0.43 to 0.87 eV with decrease of tempe- rature	-



BIG.6.35: Plot of  $\ln f_R$  against  $1/T$  for a mixture of 74 mole % of NPOOB with 26 mole % of OH-EBBA. The vertical arrow indicates  $T_{AN}$ .



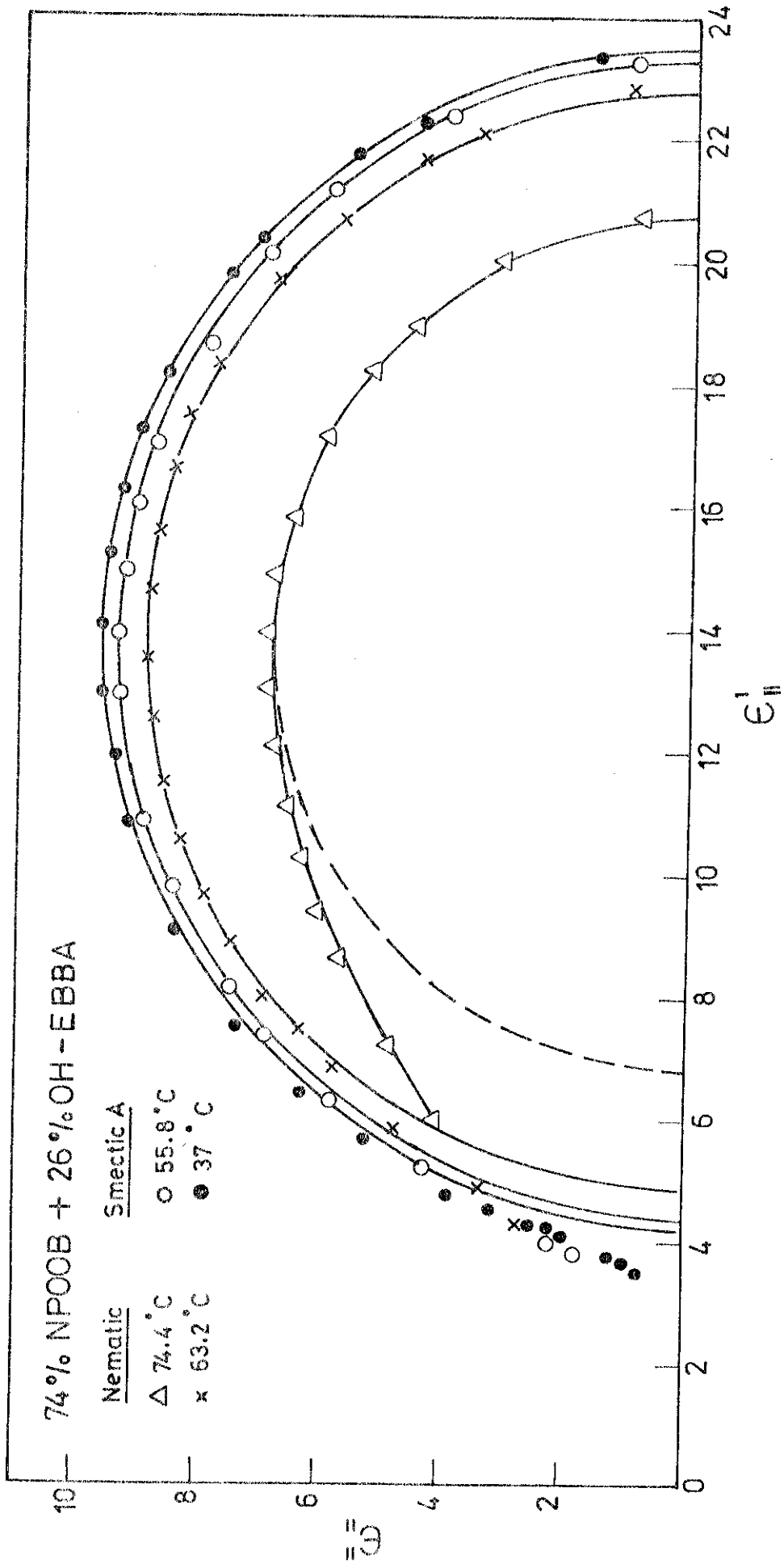


FIG. 6.34: Cole-Cole plots for  $\epsilon''$ -relaxation in the case of 74 mole percent of NPOOB and 26mole per cent of OH-EBBA at different temperatures.

- 38 L.Bata, A.Buka, I.Janossy and J.Szabon, *Advances in Liquid Crystal Research & Applications*, Ed.L.Bata, Vol.I, Pergamon, Oxford (1980) p.209.
- 39 A. Buka, P.G.Owen and A.H.Price, *Mol.Cryst.Liq.Cryst.* 51, 273 (1979).
- 40 A.H.Price and M.W.Evans, *J.Chem.Soc. Faraday II*, 76, 217 (1980).
- 41 G.J.F.Botcher and P.Bordewijk, *Theory of Electric Polarization*, Vol.2, Elsevier Scientific Publishing Co., Amsterdam (1978).
- 42 D.M.S.Edwards and P.A.Madden, *Mol.Phys.* 48, 471 (1983).
- 43 A.Mircea-Roussel, L.Leger, F.Rondelez and W.H.de Jeu, *J.de Phys.* 36, C1-93 (1975).
- 44 F.Rondelez, *Contribution a l'etude des effets de champs dans les cristaux liquides nematiques et cholesteriques*, Ph.D. Thesis, University of Paris-Sud Orsay (1973).
- 45 F.Schneider, *Z.Naturforsch* 33a, 601 (1978).